

Controlling the False Discovery Rate in Transformational Sparsity: Split Knockoffs

Yang Cao[†], Xinwei Sun[‡] and Yuan Yao[†]

[†]Hong Kong University of Science and Technology, [‡]Fudan University

Abstract

Controlling the False Discovery Rate (FDR) in a variable selection procedure is critical for reproducible discoveries, which receives an extensive study in sparse linear models. However, in many scenarios, the sparsity constraint is not directly imposed on the parameters, but on a linear transformation of the parameters to be estimated. Examples can be found in total variations, wavelet transforms, fused LASSO, and trend filtering, etc. In this paper, we propose a data adaptive FDR control in this transformational sparsity setting, the Split Knockoff method. The proposed scheme exploits both variable and data splitting. By variable splitting, the linear transformation constraint is relaxed to its Euclidean proximity in a lifted parameter space, yielding an orthogonal design for improved power and orthogonal Split Knockoff copies. Moreover, by randomly splitting the data into two independent subsets, new knockoff statistics are generated with signs as independent Bernoulli random variables, enabling inverse supermartingale constructions for provable FDR control. Simulation experiments show that the proposed methodology achieves desired FDR and power. An application to Alzheimer’s Disease study is provided that atrophy brain regions and their abnormal connections can be discovered based on a structural Magnetic Resonance Imaging dataset (ADNI).

Contents

1	Introduction	3
1.1	Organization of the paper	5
2	The Split Knockoff Method	6
2.1	Data Splitting and Intercept Estimation on the First Dataset	6
2.2	Construction of Knockoff Matrix with the Second Dataset	7
2.3	Feature and Knockoff Significance	7
2.4	Three Types of Split Knockoff Statistics	8

3 FDR Control of Split Knockoffs	9
3.1 Case I: Split Knockoff Statistics	11
3.2 Case II: Barber-Candès Type Statistics	13
4 Power and Path Consistency for Split LASSO	15
4.1 ν -Incoherence Condition for Split LASSO	15
4.2 Path Consistency and Power	16
5 Simulation Experiment	16
5.1 Experimental Setting	17
5.2 Performances of Split Knockoffs	18
5.3 Comparisons between Split Knockoffs and Knockoffs	18
6 Application: Alzheimer’s Disease	20
6.1 Dataset	21
6.2 Region Selection	22
6.3 Connection Selection	23
7 Discussion	24
7.1 Generalized LASSO and Knockoffs	24
7.2 Failure of Exchangeability in Split Knockoffs	25
8 Conclusion	26
A Construction of Split Knockoff Copies	31
B Proof for Theorem 3.1	32
B.1 Proof for Theorem 3.1: Case I	34
B.2 Proof for Theorem 3.1: Case II	36
C Proof for Key Lemmas	38
C.1 Proof for Lemma 3.2 (Lemma B.1)	39
C.2 Proof for Lemma 3.3 (Lemma B.2)	42
C.3 Proof for Lemma 3.4 (Lemma B.3)	43
D Proof for Theorem 4.1	44
D.1 Primal-Dual Witness Property	45
D.2 Incoherence Condition and Path Consistency	45
E Supplementary Materials for Alzheimer’s Disease Experiments	47
E.1 Names and Abbreviations in Automatic Anatomical Labeling (AAL) Atlas	48
E.2 Parameter Importance Index as Selection Frequency	48

1 Introduction

Variable selection or sparse model selection is a fundamental problem in statistical research. Equipped with the wide spread of modern data acquisition facilities, one can simultaneously measure a large number of covariates or features and it is desired to discover a relatively small amount of dominant factors governing the variations. In many scenarios, such a sparsity constraint does not always rely on a small number of measured covariates or features, but is about some transformations, often linear, of parameters. For instance, in signal processing such as images, sparsity of edges or jumps lies in wavelet transforms (Donoho and Johnstone, 1995) or total variations (Rudin et al., 1992; Cai et al., 2012); in statistical ranking, sparsity of graph gradients disclose the partial orders or candidate groups in ties (Huang et al., 2016, 2020); in genomic studies of human cancer, sparsity in 1-D fused LASSO (Tibshirani et al., 2005) is associated with abnormality of copy numbers of genome orders in comparative genomic hybridization (CGH) data, a valuable way of understanding human cancer; in trend filtering (Kim et al., 2009), sparsity lies in the change point detection of piece-wise linear time series.

In this paper, consider the following transformational sparsity or structural sparsity problem in linear regression where a linear transformation of parameters is sparse.

$$y = X\beta^* + \varepsilon, \quad \gamma^* = D\beta^*, \quad (1)$$

where $y \in \mathbb{R}^n$ is the response vector, $X \in \mathbb{R}^{n \times p}$ is the design matrix, $\beta^* \in \mathbb{R}^p$ is the unknown coefficient vector, $\varepsilon \sim \mathcal{N}(0, \sigma^2 I_n)$ is Gaussian noise; $D \in \mathbb{R}^{m \times p}$ is the linear transformer, and $\gamma^* \in \mathbb{R}^m$ is the sparse vector. And the target for this model is to recover the support set of γ^* . For shorthand notations, we define the nonnull set $S_1 = \text{supp}(\gamma^*) = \{i : \gamma_i^* \neq 0\}$, and the null set $S_0 = \{i : \gamma_i^* = 0\}$. Note that if we take $m = p$ and $D = I_p$, this model is degenerated into the standard sparse linear regression, therefore, this model can be viewed as a generalization for the traditional sparse regression problem.

Example. Considering brain imaging data analysis for Alzheimer’s Disease, y represents the Alzheimer’s Disease Assessment Scale (ADAS) of patients, $X_{i,j}$ measures the gray matter volume of brain region j in the cerebrum brain of subject i . Taking the identity matrix $D = I$ (where $m = p = 90$), one searches for highly atrophy brain regions for AD; taking D as the graph gradient operator on the brain region connectivity graph (where $m = 463 > p = 90$), abnormal connections of brain regions due to disease are discovered. Sparsity associated with various linear transformations above discloses both important lesion regions that undergo severe damages in disease progression and highly differential connections that link stable regions to Hippocampus, one of the most important regions accounting for Alzheimer’s Disease (Juottonen et al., 1999). Such discoveries using the methodology in this paper are illustrated by Figure 1, whose details will be discussed in Section 6.

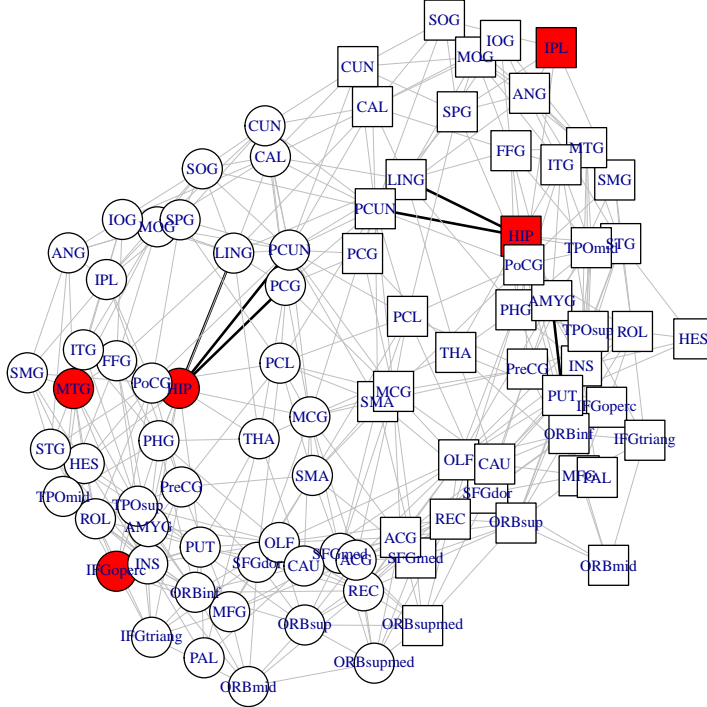


Figure 1: Selected brain regions and connections in Alzheimer’s Disease. Each vertex represents a Cerebrum brain region in Automatic Anatomical Labeling (AAL) atlas (Tzourio-Mazoyer et al., 2002), whose abbreviations and full names are provided in Table 4. Here, vertices with a circle shape represent the Left brain regions, while the ones with a square shape represent the Right brain regions. An edge connects two vertices if and only if the associated two brain regions are adjacent. The method in this paper selects red vertices as significantly degenerate lesion regions and bold edges for highly differential connections.

To evaluate the accuracy of an empirically discovered set \hat{S} of non-null parameters, the false discovery rate (FDR) is the goal of this paper in favor of the reproducibility of discoveries. Formally speaking, FDR of a selection set \hat{S} is defined as

$$\text{FDR} = \mathbb{E} \left[\frac{|\{i : i \in \hat{S} \cap S_0\}|}{|\hat{S}| \vee 1} \right]. \quad (2)$$

The problem of controlling FDR has been widely studied since Benjamini and Hochberg (1995). In particular, Barber et al. (2015) recently proposed the knock-off method for sparse linear regression when $D = I_p$ with a theoretical guarantee of the upper bound of FDR. This work can be further applied to group sparse model, multi-task regression model (Dai and Barber, 2016), Huber’s robust regression for out-

lier detection (Xu et al., 2016), and high dimensional scenarios (Barber et al., 2019). In particular, Candès et al. (2018) proposed Model-X knockoff for random design and showed in (Barber et al., 2020) that Model-X knockoff is robust to estimation error of random design parameters. Combined with generative adversarial networks, deep knockoff (Romano et al., 2019) is developed for nonparametric random designs. Moreover, side information is considered in Ren and Candès (2020) and derandomized Knockoffs are proposed in Ren et al. (2021). However, for general constraint $\gamma = D\beta$, it is not clear how to apply such knockoff methods to transformational sparsity except for some special cases which can be reduced to sparse linear regression (see Section 7.1 for details).

To fill in this gap, a data adaptive selection for the transformational sparsity problem is proposed in this paper by developing a new method in the framework of knockoffs, the Split Knockoff method. In our approach, the linear submanifold constraint $\gamma = D\beta$ is relaxed into its Euclidean ν -proximity or neighbourhood, known as the variable splitting technique in optimization. It leads to an orthogonal design as well as orthogonal knockoff copies. To overcome the challenge of exchangeability failure, the whole dataset is further split into two independent subsets, with β being estimated on one and sparse γ selected on the other with new designs of Split Knockoff statistics. Equipped with orthogonal Split Knockoff copies, the crucial new statistics design has signs as independent Bernoulli random variables, decoupled from magnitudes, that enables the inverse supermartingale inequalities to guarantee the FDR control. It also enables us to handle some traditional type of knockoff statistics whose signs and magnitudes are dependent, via filtration refinement. The ν -relaxation above can be used for power optimization as a trade-off between incoherence improvement and loss of weak signals. The methodology is validated by simulation experiments and applied to the study of Alzheimer’s Disease, where atrophy brain regions and their abnormal connections are successfully discovered.

1.1 Organization of the paper

- In Section 2, we introduce the methodology of Split Knockoffs.
- In Section 3, the FDR of Split Knockoffs is shown under control, with an outline on how to achieve this by developing some new inverse supermartingale constructions.
- In Section 4, the influence of ν -relaxation on the power of Split Knockoffs is discussed, through the path consistency property of Split LASSO regularization paths.
- In Section 5, simulation experiments are conducted with a comparison of the performance of Split Knockoffs in terms of FDR and power.

- In Section 6, Alzheimer’s Disease is studied based on brain imaging data, where Split Knockoffs discovers the abnormal lesion regions and their connections in brains.
- In Section 7, we discuss why Knockoffs with generalized LASSO fail in general settings of transformational sparsity, and the main challenge in establishing theoretical FDR control of Split Knockoffs, the failure of exchangeability.
- In Section 8, conclusions and future directions are discussed.

Details for proofs, as well as additional results on the application of Alzheimer’s disease are provided in supplementary material sections.

2 The Split Knockoff Method

Inspired by the variable splitting in Boosting with structural sparsity (Huang et al., 2020), our first key treatment lies in the relaxation of linear constraint $\gamma = D\beta$ to its Euclidean ν -proximity (neighbourhood) as an unconstrained optimization, called as Split LASSO here,

$$\min_{\beta, \gamma} \frac{1}{2n} \|y - X\beta\|_2^2 + \frac{1}{2\nu} \|D\beta - \gamma\|_2^2 + \lambda \|\gamma\|_1, \quad \lambda > 0, \quad (3)$$

where $\nu > 0$ is a parameter to control the Euclidean gap between $D\beta$ and γ . In other words, we shall allow model parameters varied in the neighborhood of the linear subspace $D\beta = \gamma$, where the larger is ν , the larger is the relaxation proximity. In the lifted parameter space (β, γ) , the ν -relaxation renders an orthogonal design (identity matrix) for γ , improving the incoherence condition for power, which is sufficient and necessary to identify nonnull features in the presence of noise (see Section 4 for details). Moreover, it leads to orthogonal Split Knockoff features for FDR control.

Another key element in our methodology is that, instead of using the whole dataset, we randomly split the data into two independent subsets, with one to estimate non-sparse intercept parameter β and the other to construct knockoffs for the selection of sparse parameter γ . Such a treatment is crucial to enable independent signs of Split Knockoff statistics, as Bernoulli random variables, recovering inverse supermartingale structures for provable FDR control.

The detailed procedure goes as follows.

2.1 Data Splitting and Intercept Estimation on the First Dataset

Data Splitting. The dataset $\mathcal{D} = (X, y)$ is randomly splitted into two subsets as $\mathcal{D}_1 = (X_1, y_1)$ and $\mathcal{D}_2 = (X_2, y_2)$ with n_1 and n_2 samples respectively, where $n_1 + n_2 = n$, and $n_2 \geq m + p$.¹

¹When this constraint is not satisfied in high dimensional settings, one can use the first dataset for screening to reduce dimension.

Estimation of Intercept ($\beta(\lambda)$) with \mathcal{D}_1 .

1. Either compute the Split LASSO regularization path (3) as a bounded continuous function with respect to λ , i.e. $\beta(\lambda)$, implicitly assuming its dependence on ν throughout the paper, based on the first dataset $\mathcal{D}_1 = (X_1, y_1)$.
2. Or alternatively, to maximize the power, one can take $\beta(\lambda) = \hat{\beta}_{\hat{\lambda}, \hat{\nu}}$ as an optimal estimator with minimal cross validation loss — with respect to the parameter λ and ν — on the Split LASSO path.

2.2 Construction of Knockoff Matrix with the Second Dataset

Now we construct fake knockoff features based on the second dataset $\mathcal{D}_2 = (X_2, y_2)$. For this purpose, the transformational sparsity model (1) on the second dataset $\mathcal{D}_2 = (X_2, y_2)$ can be rewritten as the following linear regression in the lifted parameter (β^*, γ^*) space with heterogeneous noise:

$$\tilde{y} = A_\beta \beta^* + A_\gamma \gamma^* + \tilde{\varepsilon}, \quad (4)$$

where we denote ε_2 to be the Gaussian noise in y_2 and

$$\tilde{y} = \begin{pmatrix} \frac{y_2}{\sqrt{n_2}} \\ 0_m \end{pmatrix}, \quad A_\beta = \begin{pmatrix} \frac{X_2}{\sqrt{n_2}} \\ \frac{D}{\sqrt{\nu}} \end{pmatrix}, \quad A_\gamma = \begin{pmatrix} 0_{n_2 \times m} \\ -\frac{I_m}{\sqrt{\nu}} \end{pmatrix}, \quad \tilde{\varepsilon} = \begin{pmatrix} \frac{\varepsilon_2}{\sqrt{n_2}} \\ 0_m \end{pmatrix}. \quad (5)$$

Knockoff Construction on \mathcal{D}_2 . The split knockoff copy matrix \tilde{A}_γ satisfies

$$\tilde{A}_\gamma^T \tilde{A}_\gamma = A_\gamma^T A_\gamma, \quad A_\beta^T \tilde{A}_\gamma = A_\beta^T A_\gamma, \quad A_\gamma^T \tilde{A}_\gamma = A_\gamma^T A_\gamma - \text{diag}(s), \quad (6)$$

where $s \in \mathbb{R}^m$ is some non-negative vector. Since the original features A_γ is an orthogonal design, the Split Knockoff matrix, \tilde{A}_γ , is thus an orthogonal matrix, that imitates the inner product or angles of features in A_γ , but are different to the original features as much as possible. In particular, the existence of the nonsparse intercept features further require that \tilde{A}_γ imitates the inner product or angles between A_γ and A_β . Explicit solutions of Equation (6) when $n_2 \geq m + p$ are discussed in Section A. For convenience, \tilde{A}_γ is partitioned according to that of A_γ , $\tilde{A}_\gamma^T = (\tilde{A}_{\gamma,1}^T; \tilde{A}_{\gamma,2}^T)^T$, i.e. $\tilde{A}_{\gamma,1} \in \mathbb{R}^{n_2 \times m}$ is the submatrix consisting of the first n_2 rows of \tilde{A}_γ and $\tilde{A}_{\gamma,2} \in \mathbb{R}^{m \times m}$ is the remaining submatrix.

2.3 Feature and Knockoff Significance

Given $(\tilde{y}, A_\beta, A_\gamma, \tilde{A}_\gamma)$ and $\beta(\lambda)$, we are now ready to compute Feature and Knockoff significance statistics.²

²Here, we compute the regularization paths on A_γ and \tilde{A}_γ separately rather than jointly, which can lower the computational cost at lower dimensionality.

Feature Significance (Z) on \mathcal{D}_2 .

1. Compute the Split LASSO regularization path for γ ,

$$\gamma(\lambda) := \arg \min_{\gamma} \frac{1}{2} \|\tilde{y} - A_{\beta}\beta(\lambda) - A_{\gamma}\gamma\|_2^2 + \lambda \|\gamma\|_1, \quad \lambda > 0. \quad (7)$$

2. Define the feature significance as the maximal $\lambda > 0$ on the regularization path $\gamma_i(\lambda)$ such that $\gamma_i(\lambda)$ is nonzero for all $i \in \{1, 2, \dots, m\}$:

$$Z_i = \sup \{\lambda : \gamma_i(\lambda) \neq 0\}. \quad (8)$$

Knockoff Significance (\tilde{Z}) on \mathcal{D}_2 .

1. Compute the Split LASSO regularization path for $\tilde{\gamma}$,

$$\tilde{\gamma}(\lambda) := \arg \min_{\tilde{\gamma}} \frac{1}{2} \|\tilde{y} - A_{\beta}\beta(\lambda) - \tilde{A}_{\gamma}\tilde{\gamma}\|_2^2 + \lambda \|\tilde{\gamma}\|_1, \quad \lambda > 0. \quad (9)$$

2. Define the knockoff significance as the maximal $\lambda > 0$ on the regularization path $\tilde{\gamma}_i(\lambda)$ such that $\tilde{\gamma}_i(\lambda)$ is nonzero, for all $i \in \{1, 2, \dots, m\}$:

$$\tilde{Z}_i = \sup \{\lambda : \tilde{\gamma}_i(\lambda) \neq 0\}. \quad (10)$$

Moreover, one may apply a truncation of sign mismatch on \tilde{Z} to define a new knockoff significance statistics,

$$\tau(\tilde{Z}) := \tilde{Z} \odot \mathbf{1}\{r = \tilde{r}\} \quad (11)$$

where the symbol \odot stands for Hadamard product, $r_i := \lim_{\lambda \rightarrow Z_i - 0} \text{sign}(\gamma_i(\lambda))$ and $\tilde{r}_i := \lim_{\lambda \rightarrow \tilde{Z}_i - 0} \text{sign}(\tilde{\gamma}_i(\lambda))$. Such a truncation sets zeroes those knockoff significance values if their signs differ to their associated feature significance values. As we shall see later in this paper, the truncated knockoff significance may reduce the conservativeness in selections compared with the untruncated one.

2.4 Three Types of Split Knockoff Statistics

We introduce a family of Split Knockoff W statistics. The symbol \odot stands for Hadamard product.

Split Knockoff Statistics.

1. $W^S := Z \odot \text{sign}(Z - \tilde{Z})$, where S refers to “Split”.
2. $W^{S\tau} := Z \odot \text{sign}(Z - \tau(\tilde{Z}))$, where $S\tau$ refers to applying truncation (11) on W^S .
3. $W^{BC} := (Z \vee \tilde{Z}) \odot \text{sign}(Z - \tilde{Z})$, where BC refers to the original definition adopted by Barber-Candès in [Barber et al. \(2015\)](#).

All the three versions will be handled in a unified framework in this paper. As to FDR, they are all under the control; while the difference lies in power. Ideally W^S and $W^{S\tau}$ achieve higher power compared with W^{BC} , though their differences in practice might not be significant. For shorthand notation, we use W^* to represent any one in the family, where $\star \in \{S, S\tau, BC\}$. In all cases, as we wish to select i when W_i^* is large and positive. Let q be our target FDR, two data-dependent threshold rules based on a pre-set nominal level q are defined as

$$(\text{Split Knockoff}) \quad T_q^* = \min \left\{ \lambda : \frac{|\{i : W_i^* \leq -\lambda\}|}{1 \vee |\{i : W_i^* \geq \lambda\}|} \leq q \right\},$$

$$(\text{Split Knockoff+}) \quad T_q^* = \min \left\{ \lambda : \frac{1 + |\{i : W_i^* \leq -\lambda\}|}{1 \vee |\{i : W_i^* \geq \lambda\}|} \leq q \right\},$$

or $T_q^* = +\infty$ if this set is empty. And in all cases, the selector is defined as

$$\hat{S}^* = \{i : W_i^* \geq T_q^*\}.$$

3 FDR Control of Split Knockoffs

In this section, we first show that the false discovery rates are under control for the Split Knockoff method, then present the key ideas on how to reach this analysis.

To be specific, the following theorem of FDR control is established for all the Split Knockoff selectors. For Split Knockoff, we control a “modified” FDR as [Barber et al. \(2015\)](#) that adds q^{-1} in the denominator, which should have little effect if a large number of features are selected; for Split Knockoff+, we get the exact FDR control.

Theorem 3.1 (FDR Control of Split Knockoffs). *For all $0 < q \leq 1$, $\star \in \{S, S\tau, BC\}$, and all $\nu > 0$, there holds*

(a) *(Modified FDR of Split Knockoff)*

$$\mathbb{E} \left[\frac{|\{i : i \in \hat{S}^* \cap S_0\}|}{|\hat{S}^*| + q^{-1}} \right] \leq q.$$

(b) (FDR of Split Knockoff+)

$$\mathbb{E} \left[\frac{\left| \{i : i \in \hat{S}^* \cap S_0\} \right|}{\left| \hat{S}^* \right| \vee 1} \right] \leq q.$$

Since the FDR is uniformly under control for all $\nu > 0$, the hyperparameter ν from Split LASSO can be used to optimize the power of Split Knockoffs. The influence of ν on power is of two folds (see Section 4 for more details). On one hand, increasing ν may increase the power of discovering strong nonnull features whose magnitudes are large. It is because that enlarging ν will improve the incoherence condition of the Split LASSO such that strong nonnull features will appear earlier on the path than the weak ones and nulls. On the other hand, increasing ν may lose the power of discovering weak nonnull features whose magnitudes are below ν and the noise scale. Therefore a trade-off of these two aspects will lead to a good power by optimizing ν , which can be achieved empirically by cross-validation as what we describe in intercept estimation $\hat{\beta}$. Performance of such a choice will be confirmed in simulation experiments in Section 5.

The main challenge in establishing the FDR control of Split Knockoffs lies in the failure of exchangeability (see Section 7.2 for more discussions). Such a failure leads to dependency between the magnitude and sign of the original type of W statistics (W^{BC}), which further fails the inverse supermartingale argument in Barber et al. (2015, 2019) for provable FDR control. To overcome this challenge, our key technical development is based on the orthogonal design and the rendered orthogonal Split Knockoff copies, which together with data splitting leads to independent Bernoulli processes for signs of W^S and $W^{S\tau}$, decoupled or independent to their magnitudes. This enables us some new inverse supermartingale structures such that the FDR control can be proved, in a similar way to Barber et al. (2019). Furthermore, W^S enjoys a particularly nice structure that its associated inverse supermartingale has a more refined filtration than that of W^{BC} , which enables us to reach an upper bound for W^{BC} via W^S . Below we will present the key ideas in details for the FDR control.

First of all, following the standard steps in knockoffs as in Barber et al. (2015), we can transfer the problem of bounding FDR by q in Theorem 3.1 into the problem of bounding $\mathbb{E} [\mathcal{M}_{T_q}(W^*)]$ by one (see Section B for details), where

$$\mathcal{M}_T(W^*) = \frac{\sum_{i \in S_0} 1\{W_i^* \geq T\}}{1 + \sum_{i \in S_0} 1\{W_i^* \leq -T\}}.$$

Next, we will handle the split knockoff statistics W^S and the Barber-Candès type statistics W^{BC} in two cases, respectively, while the analysis on the sign-mismatch truncated statistics $W^{S\tau}$ can be done in a similar way as W^S . The section is organized as following:

1. An inverse supermartingale structure on $\mathcal{M}_T(W^S)$ is introduced, which enables the optional stopping theorem to bound $\mathbb{E} [\mathcal{M}_{T_q^S}(W^S)]$, in Section 3.1.

2. Barber-Candès type of knockoff statistics W^{BC} renders a coarser filtration than W^S , which enables $\mathbb{E} \left[\mathcal{M}_{T_q^{\text{BC}}}(W^S) \right]$ providing an upper bound of $\mathbb{E} \left[\mathcal{M}_{T_q^{\text{BC}}}(W^{\text{BC}}) \right]$, in Section 3.2.

3.1 Case I: Split Knockoff Statistics

The key property of split knockoff statistics W^S lies in that its magnitudes $|W^S|$ are independent to its signs $\{\text{sign}(W^S)\}$, and the signs $\{\text{sign}(W_i^S)\}$ are independent Bernoulli random variables which enables us to construct an inverse supermartingale.

We start from the Karush–Kuhn–Tucker (KKT) conditions of Eq. (7) and Eq. (9). From Eq. (7) and Eq. (9), the KKT conditions that the solution $\gamma(\lambda)$, $\tilde{\gamma}(\lambda)$ with respect to $\lambda > 0$ should satisfy is

$$\lambda \rho(\lambda) + \frac{\gamma(\lambda)}{\nu} = \frac{D\beta(\lambda)}{\nu}, \quad (12a)$$

$$\lambda \tilde{\rho}(\lambda) + \frac{\tilde{\gamma}(\lambda)}{\nu} = \frac{D\beta(\lambda)}{\nu} + \underbrace{\left\{ -\text{diag}(s)\gamma^* + \frac{\tilde{A}_{\gamma,1}^T}{\sqrt{n_2}}\varepsilon_2 \right\}}_{=:\zeta}, \quad (12b)$$

where $\rho(\lambda) \in \partial\|\gamma(\lambda)\|_1$, $\tilde{\rho}(\lambda) \in \partial\|\tilde{\gamma}(\lambda)\|_1$, ε_2 is the Gaussian noise in y_2 and $\tilde{A}_{\gamma,1} \in \mathbb{R}^{n_2 \times m}$ is the submatrix of \tilde{A}_γ as the first n_2 rows. For shorthand notations, define $\zeta := -\text{diag}(s)\gamma^* + \frac{\tilde{A}_{\gamma,1}^T}{\sqrt{n}}\varepsilon_2$.

Now we are ready to show that the magnitudes $|W^S|$ are independent to the signs $\text{sign}(W^S)$. Note that $\beta(\lambda)$ is determined from the first dataset $\mathcal{D}_1 = (X_1, y_1)$, whence independent to the second dataset $\mathcal{D}_2 = (X_2, y_2)$ and particularly ζ . Therefore, it suffices to consider the random variable ζ conditional on a predetermined $\beta(\lambda)$. From Eq. (12a), $\gamma(\lambda)$ is determined by $\beta(\lambda)$ and thus independent to ζ , so is $|W^S| = Z$ as a function of $\gamma(\lambda)$. On the other hand from Eq. (12b), conditional on a determined $\beta(\lambda)$, $\tilde{\gamma}(\lambda)$ as well as \tilde{Z} , are determined by ζ from $\mathcal{D}_2 = (X_2, y_2)$. Therefore, $|W^S|$, determined by $\beta(\lambda)$ on $\mathcal{D}_1 = (X_1, y_1)$, is independent to $\text{sign}(W^S) = \text{sign}(Z - \tilde{Z})$, depending on ζ with $\mathcal{D}_2 = (X_2, y_2)$.

To see that the signs $\{\text{sign}(W^S)\}$ are independent Bernoulli random variables, ζ follows an independently joint Gaussian distribution as a result of the orthogonal Split Knockoff matrix satisfying (6) (see Eq. (42) in Section C for details), *i.e.*

$$\zeta \sim \mathcal{N} \left(-\text{diag}(s)\gamma^*, \frac{1}{n_2} \text{diag}(s)(2I_m - \text{diag}(s)\nu)\sigma^2 \right).$$

Then we have the following lemma.

Lemma 3.2. *Given any determined $\beta(\lambda)$, $|W^S| = Z$ are determined, with $\text{sign}(W^S)$ determined by ζ . Then $\{W_i^S < 0\}$ are some independent Bernoulli random variables.*

Furthermore, for $i \in S_0$, there holds

$$\mathbb{P}[1\{W_i^S < 0\} = 1] \geq \frac{1}{2}.$$

Remark. In particular, for the case of split knockoff statistics with sign-mismatch truncation $W^{S\tau}$, there holds $\mathbb{P}[1\{W_i^{S\tau} < 0\} = 1] = \frac{1}{2}$ for $i \in S_0$.

This lemma states that given $|W^S| = Z$, $\text{sign}(W^S)$ consists of independent random variables with $\mathbb{P}[W^S < 0] \geq 1/2$ on the nulls. With such a property, we can construct an inverse supermartingale whose optional stopping theorem gives an upper bound on $\mathbb{E}[\mathcal{M}_{T_q^S}(W^S)]$.

For simplicity, we rearrange the index of W^S , such that $|W_{(1)}^S| \geq |W_{(2)}^S| \geq \dots \geq |W_{(m^*)}^S|$ for $\{(1), (2), \dots, (m^*)\} = S_0$, where $m^* = |S_0| \leq m$. Further denote $B_{(i)} = 1\{W_{(i)}^S < 0\}$, then there holds

$$\begin{aligned} \frac{\sum_{i \in S_0} 1\{W_i^S \geq T_q^S\}}{1 + \sum_{i \in S_0} 1\{W_i^S \leq -T_q^S\}} &= \frac{1 + \sum_{i \in S_0} 1\{|W_i^S| \geq T_q^S\}}{1 + \sum_{i \in S_0} 1\{|W_i^S| \geq T_q^S, W_i^S < 0\}} - 1, \\ &= \frac{1 + J}{1 + B_{(1)} + B_{(2)} + \dots + B_{(J)}} - 1, \end{aligned} \quad (13)$$

where $J \leq m^*$ is defined to be the index satisfying

$$|W_{(1)}^S| \geq |W_{(2)}^S| \geq \dots \geq |W_{(J)}^S| \geq T_q^S > |W_{(J+1)}^S| \geq \dots \geq |W_{(m^*)}^S|,$$

in other words, $J = \text{argmax}_{k \leq m^*} \{|W_{(k)}^S| \geq T_q^S\}$. The following lemma summarizes the inverse supermartingale inequality, which gives an upper bound for the Eq. (13).

Lemma 3.3. *Given any determined $\beta(\lambda)$, let $\{G_i\}_{i=1}^m$ be some proper Borel sets such that $B_i = 1\{\zeta_i \in G_i\}$ with $\mathbb{P}[B_i = 1] = \rho_i$. Let $\rho > 0$ satisfying $\rho \leq \min_i \{\rho_i\}$. Let J be a stopping time with respect to the filtration $\{\mathcal{F}_j\}_{j=1}^m$ in inverse time defined as*

$$\mathcal{F}_j = \sigma \left(\left\{ \sum_{i=1}^j B_{(i)}, \zeta_{(j+1)}, \dots, \zeta_{(m)} \right\} \right)$$

Then

$$\mathbb{E} \left[\frac{1 + J}{1 + B_{(1)} + B_{(2)} + \dots + B_{(J)}} \right] \leq \rho^{-1}.$$

One can verify that $J = \text{argmax}_{k \leq m^*} \{|W_{(k)}^S| \geq T_q^S\}$ is indeed a stopping time with respect to the filtration $\{\mathcal{F}_j\}_{j=1}^m$ in inverse time. Applying Lemma 3.3 to Eq. (13) with the property that $\mathbb{P}[B_i = 1] \geq \rho = 1/2$ for $i \in S_0$ as shown in Lemma 3.2, we reach our desired result. The same procedure can be applied to the case of $W^{S\tau}$.

3.2 Case II: Barber-Candès Type Statistics

The nice properties of W^S provide us a bridge to the analysis of W^{BC} . In order to apply the inverse martingale inequality for $\mathcal{M}_T(W^S)$ to bound $\mathcal{M}_T(W^{BC})$, below we are going to show that

- (a) $\mathcal{M}_T(W^S)$ provides an upper bound for $\mathcal{M}_T(W^{BC})$, that $\mathcal{M}_T(W^{BC}) \leq \mathcal{M}_T(W^S)$;
- (b) The inverse supermartingale associated with $\mathcal{M}_T(W^S)$ has a more refined filtration than that of $\mathcal{M}_T(W^{BC})$ such that stopping time T_q^{BC} is also a stopping time of the former.

Recall that by definitions of W^{BC} and W^S , there holds for all $i \in \{1, 2, \dots, m\}$ that

- (i) $\{i : W_i^{BC} > 0\} = \{i : W_i^S > 0\}$, on which $|W_i^{BC}| = Z_i = |W_i^S|$;
- (ii) $\{i : W_i^{BC} < 0\} = \{i : W_i^S < 0\}$, on which $|W_i^{BC}| = \tilde{Z}_i > Z_i = |W_i^S|$.

To see point (a), (i) implies $\{i \in S_0 : W_i^{BC} \geq T\} = \{i \in S_0 : W_i^S \geq T\}$, and (ii) says $\{i \in S_0 : W_i^S \leq -T\} \subset \{i \in S_0 : W_i^{BC} \leq -T\}$, which further indicates

$$\mathcal{M}_T(W^{BC}) = \frac{\sum_{i \in S_0} 1\{W_i^{BC} \geq T\}}{1 + \sum_{i \in S_0} 1\{W_i^{BC} \leq -T\}} \leq \frac{\sum_{i \in S_0} 1\{W_i^S \geq T\}}{1 + \sum_{i \in S_0} 1\{W_i^S \leq -T\}} =: \mathcal{M}_T(W^S). \quad (14)$$

Thus $\mathcal{M}_T(W^S)$ offers an upper bound for $\mathcal{M}_T(W^{BC})$.

It remains to validate point (b). Below we show that, the filtration associated with $\mathcal{M}_T(W^{BC})$ is a refinement of the filtration associated with $\mathcal{M}_T(W^S)$, hence a stopping time adapted to the latter is also adapted to the former.

Specifically, consider the filtrations in inverse time

$$\begin{aligned} \mathcal{F}^{BC}(T) &= \sigma(\#\{i : W_i^{BC} \geq T\}, \#\{i : W_i^{BC} \leq -T\}, \{\zeta_i : |W_i^{BC}| < T\}), \\ \mathcal{F}^S(T) &= \sigma(\#\{i : W_i^S \geq T\}, \#\{i : W_i^S \leq -T\}, \{\zeta_i : |W_i^S| < T\}). \end{aligned}$$

We are going to show that $\mathcal{F}^{BC}(T) \subseteq \mathcal{F}^S(T)$, i.e. $\mathcal{F}^S(T)$ is a refined filtration of $\mathcal{F}^{BC}(T)$.

To see this, recall that by definitions of W^{BC} and W^S , from (i) we see $\{i : W_i^{BC} > 0\} = \{i : W_i^S > 0\}$, on which $|W_i^{BC}| = Z_i = |W_i^S|$, hence

$$\#\{i : W_i^{BC} \geq T\} = \#\{i : W_i^S \geq T\};$$

from (i) and (ii) we see for all i , $|W_i^S| \leq |W_i^{BC}|$, hence

$$\{\zeta_i : |W_i^{BC}| < T\} \subseteq \{\zeta_i : |W_i^S| < T\}.$$

Now it remains to consider $\#\{i : W_i^{\text{BC}} \leq -T\}$. In fact,

$$\begin{aligned}\{i : W_i^{\text{BC}} \leq -T\} &= \{i : W_i^{\text{BC}} \leq -T, |W_i^{\text{S}}| \geq T\} \cup \{i : W_i^{\text{BC}} \leq -T, |W_i^{\text{S}}| < T\}, \\ &= \{i : W_i^{\text{BC}} \leq -T, W_i^{\text{S}} \leq -T\} \cup \{i : W_i^{\text{BC}} \leq -T, |W_i^{\text{S}}| < T\}, \\ &= \{i : W_i^{\text{S}} \leq -T\} \cup \{i : W_i^{\text{BC}} \leq -T, |W_i^{\text{S}}| < T\},\end{aligned}$$

which implies that $\#\{i : W_i^{\text{BC}} \leq -T\}$ can be sufficiently determined by $\#\{i : W_i^{\text{S}} \leq -T\}$ and $\{\zeta_i : |W_i^{\text{S}}| < T\}$, both of which are already included in $\mathcal{F}^{\text{S}}(T)$. This finally shows that $\mathcal{F}^{\text{BC}}(T) \subseteq \mathcal{F}^{\text{S}}(T)$.

Therefore, a stopping time T_q^{BC} adapted to filtration $\mathcal{F}^{\text{BC}}(T)$ must be also a stopping time adapted to filtration $\mathcal{F}^{\text{S}}(T)$.

Precisely, T_q^{BC} induces the following discrete stopping time adapted to filtration $\mathcal{F}^{\text{S}}(T)$ in reverse time. For shorthand notations, we rearrange the index of W^{S} , such that $|W_{(1)}^{\text{S}}| \geq |W_{(2)}^{\text{S}}| \geq \dots \geq |W_{(m^*)}^{\text{S}}|$, where $(i) \in S_0$ and $m^* = |S_0| \leq m$. Further denote $B_{(i)} = 1\{W_{(i)}^{\text{S}} < 0\}$, then there holds

$$\begin{aligned}\frac{\sum_{i \in S_0} 1\{W_i^{\text{BC}} \geq T_q^{\text{BC}}\}}{1 + \sum_{i \in S_0} 1\{W_i^{\text{BC}} \leq -T_q^{\text{BC}}\}} &\leq \frac{\sum_{i \in S_0} 1\{W_i^{\text{S}} \geq T_q^{\text{BC}}\}}{1 + \sum_{i \in S_0} 1\{W_i^{\text{S}} \leq -T_q^{\text{BC}}\}}, \\ &= \frac{1 + \sum_{i \in S_0} 1\{|W_i^{\text{S}}| \geq T_q^{\text{BC}}\}}{1 + \sum_{i \in S_0} 1\{|W_i^{\text{S}}| \geq T_q^{\text{BC}}, W_i^{\text{S}} < 0\}} - 1, \\ &= \frac{1 + J}{1 + B_{(1)} + B_{(2)} + \dots + B_{(J)}} - 1,\end{aligned}\tag{15}$$

where $J \leq m^*$ is defined to be the index satisfying

$$|W_{(1)}^{\text{S}}| \geq |W_{(2)}^{\text{S}}| \geq \dots \geq |W_{(J)}^{\text{S}}| \geq T_q^{\text{BC}} > |W_{(J+1)}^{\text{S}}| \geq \dots \geq |W_{(m^*)}^{\text{S}}|,$$

in other words, $J = \text{argmax}_{k \leq m^*} \{|W_{(k)}^{\text{S}}| \geq T_q^{\text{BC}}\}$. Lemma 3.4 characterize the property that J is a stopping time in inverse time with respect to the filtration $\mathcal{F}_j = \sigma \left(\left\{ \sum_{i=1}^j B_{(i)}, \zeta_{(j+1)}, \dots, \zeta_{(m)} \right\} \right)$ in Lemma 3.3.

Lemma 3.4. *For any determined $\beta(\lambda)$, $J = \max_{k \leq m^*} \{|W_{(k)}^{\text{S}}| \geq T_q^{\text{BC}}\}$ is a stopping time with respect to the filtration $\{\mathcal{F}_j\}_{j=1}^m$ in inverse time defined as*

$$\mathcal{F}_j = \sigma \left(\left\{ \sum_{i=1}^j B_{(i)}, \zeta_{(j+1)}, \dots, \zeta_{(m)} \right\} \right).$$

Equipped with Lemma 3.4, one can apply Lemma 3.3 on Eq. (15) with the stopping time J and get the desired result. A complete proof for Theorem 3.1 can be found in Section B, with the proofs for key lemmas in Section C.

4 Power and Path Consistency for Split LASSO

In this section, the influence of ν on the power of Split Knockoffs is studied from a perspective of the model selection consistency of Split LASSO regularization paths (3). Below we show a family of ν -incoherence conditions, under which there is an estimator on Split LASSO regularization paths which may discover nonnull features. Yet, the influence of ν exhibits two ways on such a model selection consistency. On one hand, enlarging ν increases the power of discovering strong nonnull features whose magnitudes are large, through improving the incoherence condition; on the other hand, doing so may lose the power of discovering weak nonnull features of small magnitudes.

To see this, consider the construction in Equation (7) and (9). Ideally, a nonnull feature i will appear earlier (of larger $|W_i|$) on the Split LASSO path such that $Z_i > \tilde{Z}_i$, while a null feature j will appear later (of smaller $|W_j|$) on the path such that $Z_j < \tilde{Z}_j$. Since Z_i is determined by the Split LASSO path on \mathcal{D}_1 , it is natural to ask under what conditions that an early stage of the path has no false positive and the existence of a point on the path with model selection consistency. We approach the model selection consistency of Split LASSO following the same treatment in the traditional LASSO problem (Wainwright, 2009) and Split Linearized Bregman Iterations (Huang et al., 2016, 2020). Below we are going to see the incoherence condition that is favoured by a sufficiently large ν will provide the guarantee to find the strong nonnull features, at a possible cost of losing weak nonnulls.

Define $H_\nu := I_m - \frac{D[\Sigma_X + L_D]^{-1}D^T}{\nu}$, and further denote H_ν^{11} to be the covariance matrix for S_1 , H_ν^{00} to be the covariance matrix for S_0 , and H_ν^{10}, H_ν^{01} to be the covariance matrix between S_1 and S_0 . First of all, H_ν^{11} has to be reversible, without which identifiability is impossible. For this purpose, we assume that the Split LASSO is strongly convex when being restricted on the nonnull features.

Restricted-Strongly-Convex Condition There exists some $C_{\min} > 0$, such that the smallest eigenvalue of H_ν^{11} is bounded below, *i.e.*

$$\lambda_{\min}(H_\nu^{11}) > C_{\min}. \quad (16)$$

4.1 ν -Incoherence Condition for Split LASSO

The following family of incoherence conditions parameterized by ν is critical for path consistency of Split LASSO.

ν -Incoherence Condition There exists a parameter $\chi_\nu \in (0, 1]$, such that

$$\|H_\nu^{01}[H_\nu^{11}]^{-1}\|_\infty \leq 1 - \chi_\nu. \quad (17)$$

The influence of ν on this incoherence condition is as follows. As $\nu \rightarrow \infty$, $H_\nu = I_m - \frac{1}{\nu}D[\Sigma_X + L_D]^{-1}D^T \succeq I_m - \frac{1}{\nu}D[\Sigma_X]^{-1}D^T \rightarrow I_m$, therefore $H_\nu^{01} \rightarrow 0_{|S_0| \times |S_1|}$, while $H_\nu^{11} \rightarrow I_{|S_1|}$. In this situation, the left hand side of inequality (17) drops to zero, and it satisfies the incoherence condition with arbitrarily large $\chi_\nu \rightarrow 1$.

4.2 Path Consistency and Power

Now we are ready to state our main theorem on the Split LASSO path consistency under the restricted strongly convex and ν -incoherence conditions.

Theorem 4.1. *Assume that the design matrix X and D satisfy the Restricted-Strongly-Convex condition (16) and ν -Incoherence condition (17). Let the columns of X be normalized as $\max_{i \in [1:p]} \frac{\|x_i\|_2}{\sqrt{n}} \leq 1$. Suppose the sequence of $\{\lambda_n\}$ satisfies*

$$\lambda_n > \frac{1}{\chi_\nu} \sqrt{\frac{8\sigma^2 \log m}{n}}. \quad (18)$$

Then for some $c > 0$, the following properties hold with probability $1 - 4e^{-cn\lambda_n^2}$.

1. (No-false-positive) Split LASSO has a unique solution $(\hat{\beta}, \hat{\gamma}) \in \mathbb{R}^p \times \mathbb{R}^m$ without false positives w.r.t. γ .
2. (Sign-consistency) For C_{\min} defined in Eq. (16), if there holds

$$\min_{i \in S_1} \gamma_i^* > \lambda_n \nu \left[\frac{4\sigma}{\sqrt{C_{\min}}} + \|[H_\nu^{11}]^{-1}\|_\infty \right],$$

in addition, $\hat{\gamma}$ recovers the sign of γ^* .

The influence of ν on the power can be understood from this theorem as follows: (a) for the early stage of the Split LASSO path characterized by (18), there is no false positive and only nonnull features are selected here; (b) all the strong nonnull features whose magnitudes are larger than $O(\nu\sigma\chi_\nu^{-1}\sqrt{\log m/n})$ could be selected on the path with sign consistency. Hence a sufficiently large ν will ensure the incoherence condition for path consistency such that strong nonnull features will be selected earlier on the Split LASSO path than the nulls, at the cost of possibly losing weak nonnull features below $O(\nu\sigma\chi_\nu^{-1}\sqrt{\log m/n})$. Therefore, a good power must rely on a proper choice of ν for the trade-off.

In practice, one may apply the cross validation over (ν, λ) on the Split LASSO path with subset data \mathcal{D}_1 , to maximize the power for the optimal intercept estimator $\beta(\lambda) = \hat{\beta}_{\hat{\nu}, \hat{\lambda}}$. Equipped with the FDR control for all $\nu > 0$ in Theorem 3.1, it maximizes the empirical power with a desired FDR. Such an empirical strategy will be validated by simulation experiments in Section 5 and renders satisfied results in the study of Alzheimer's Disease in Section 6.

The formal proof of this theorem will be provided in Section D.

5 Simulation Experiment

In this section, we show by several simulation experiments that our proposed Split Knockoff method performs well with transformational sparsity. Particularly, under the cross validation optimal choice of $\beta(\lambda) = \hat{\beta}_{\hat{\nu}, \hat{\lambda}}$ and $\nu = \hat{\nu}$, Split Knockoffs achieve desired FDR control and high Power in all the three choices of W .

5.1 Experimental Setting

In model (1), we generate $X \in \mathbb{R}^{n \times p}$ ($n = 500$ and $p = 100$) i.i.d. from $\mathcal{N}(0_p, \Sigma)$, where $\Sigma_{i,i} = 1$ and $\Sigma_{i,j} = c^{|i-j|}$ for $i \neq j$, with feature correlation $c = 0.5$. Define $\beta^* \in \mathbb{R}^p$ by

$$\beta_i^* := \begin{cases} 1 & i \leq 20, i \equiv 0, -1 \pmod{3}, \\ 0 & \text{otherwise.} \end{cases}$$

Then we generate n linear measurements,

$$y = X\beta^* + \varepsilon,$$

where $\varepsilon \in \mathbb{R}^n$ is generated i.i.d. from $\mathcal{N}(0, 1)$.

For transformational sparsity, we need to specify the linear transformer D such that $\gamma^* = D\beta^*$, where γ^* is sparse. Our choice of β^* has two types of transformational sparsity that leads to the following three choices of D .

- β^* is sparse with many zero elements such that we can take $D_1 = I_p$ as the identity matrix, where in this case $m = p$.
- β^* is a uni-dimensional piecewise constant function such that we can take D_2 as the 1-D graph difference operator on a line, i.e. $D_2 \in \mathbb{R}^{(p-1) \times p}$, $D_2(i, i) = 1$, $D_2(i, i+1) = -1$ for $i = 1, \dots, p-1$, where in this case $m = p-1 < p$.
- Combining both cases, β^* is a sparse piecewise constant function such that we can take $D_3 = \begin{bmatrix} D_1 \\ D_2 \end{bmatrix} \in \mathbb{R}^{(2p-1) \times p}$, where in this case $m = 2p-1 > p$.

In simulation experiments, we use `glmnet` package (Friedman et al., 2010; Simon et al., 2011) to compute regularization paths for Split LASSO, etc. For the data splitting, we randomly split the dataset $\mathcal{D} = (X, y)$ into two parts $\mathcal{D}_1 = (X_1, y_1)$ and $\mathcal{D}_2 = (X_2, y_2)$ with n_1 and n_2 samples respectively where $n_1 = 200$ and $n_2 = 300$.

For the first choice of $\beta(\lambda)$ in Section 2.1, we take $\beta(\lambda)$ as $\beta_\nu(\lambda)$, the solution path with respect to $\beta(\lambda)$ in the ν -Split LASSO regularization path with dataset $\mathcal{D}_1 = (X_1, y_1)$. For all the regularization paths calculated in Split Knockoffs, we take $\log \lambda$ from a grid between 0 and -6 with a step size $h_\lambda = 0.01$.

For the second choice of $\beta(\lambda)$ in Section 2.1, we take $\beta(\lambda)$ as a fixed cross validation optimal estimator $\hat{\beta}_{\nu, \lambda}$ in the Split LASSO path with dataset $\mathcal{D}_1 = (X_1, y_1)$, screening on $\log \nu$ from a grid between 0 and 2 with a step size 0.4, and $\log \lambda$ from a grid between 0 and -8 with a step size 0.4. For the regularization paths of feature and knockoff significance in Eq. (7) and Eq. (9), we take $\log \lambda$ from a grid between 0 and -6 with a step size $h_\lambda = 0.01$.

5.2 Performances of Split Knockoffs

In Figure 2, we plot the performances of Split Knockoffs on $\log(\nu)$ between 0 and 2 with a step size 0.2, where $\beta(\lambda)$ is taken as the solution path $\beta_\nu(\lambda)$ in the ν -Split LASSO path. In Figure 3, we plot the performances of Split Knockoffs on $\log(\nu)$ between 0 and 2 with a step size 0.2, where $\beta(\lambda)$ is taken as a fixed cross validation optimal estimator $\hat{\beta}_{\nu,\hat{\lambda}}$ on the Split LASSO paths.

In these cases, the FDR of Split Knockoffs are all under control; while the performances in the power differ from one to another. The cross validation optimal estimator choice of $\beta(\lambda) = \hat{\beta}_{\nu,\hat{\lambda}}$ shown in Figure 3, clearly improves the selection power of Split Knockoffs compared with the ν -Split LASSO solution path choice of $\beta(\lambda) = \beta_\nu(\lambda)$ shown in Figure 2.

In the family of W -statistics in Section 2.4, $W^{S\tau}$ shows a less conservative FDR and a slightly better power than the others in Figure 2, in the tested regime of ν . In particular, the average FDR of $W^{S\tau}$ is close to the nominal level in both Figure 2 and Figure 3. This meets Lemma 3.2 where a tight characterization $\mathbb{P}[W_i^{S\tau} < 0] = 1/2$ for $i \in S_0$ is given, leading to a tighter upper bound than others on $\mathcal{M}_{T_q^{S\tau}}(W^{S\tau})$ and FDR control given by Lemma 3.3.

Meanwhile, W^{BC} is more conservative compared with W^S and $W^{S\tau}$, which trades the selection power for a better empirical FDR control. Such a phenomenon is explained by our analysis in Section 3.2 that the FDR control on W^S offers an upper bound for that of W^{BC} .

Finally, we note that in these methods, as the selection power decays when ν is huge, selectors may return empty sets whose empirical false discovery is zero, whence the average FDR drops when the selection power is lost.

5.3 Comparisons between Split Knockoffs and Knockoffs

In this section, we conduct more simulation experiments on the cross validation optimal estimator choice of $\beta(\lambda) = \hat{\beta}_{\nu,\hat{\lambda}}$, which gives higher selection power compared with the ν -Split LASSO solution path choice of $\beta(\lambda) = \beta_\nu(\lambda)$, as shown in Section 5.2. Moreover, for the choice of ν in the calculation of the feature significance and knockoff significance by Eq. (7) and Eq. (9), we take the cross validation optimal choice of $\nu = \hat{\nu}$ to maximize the selection power of Split Knockoffs.

Below, we will show the performances of Split Knockoffs with the above choice of $\beta(\lambda)$ and ν under the simulation settings described in Section 5.1. We also provide comparisons between Split Knockoffs and Knockoffs when both are applicable (the case of D_1 and D_2). In particular, for the 1-D fused LASSO case that $D_2 \in \mathbb{R}^{(p-1) \times p}$ is the graph difference operator for a line, we make Knockoffs applicable by introducing the induced LASSO problem from the generalized LASSO problem (see discussions in Section 7.1 for details). The performances of Knockoffs and Split Knockoffs with all the three choices of W statistics are presented in Table 1.

As shown in Table 1, Split Knockoffs(+) with the cross validation optimal choice

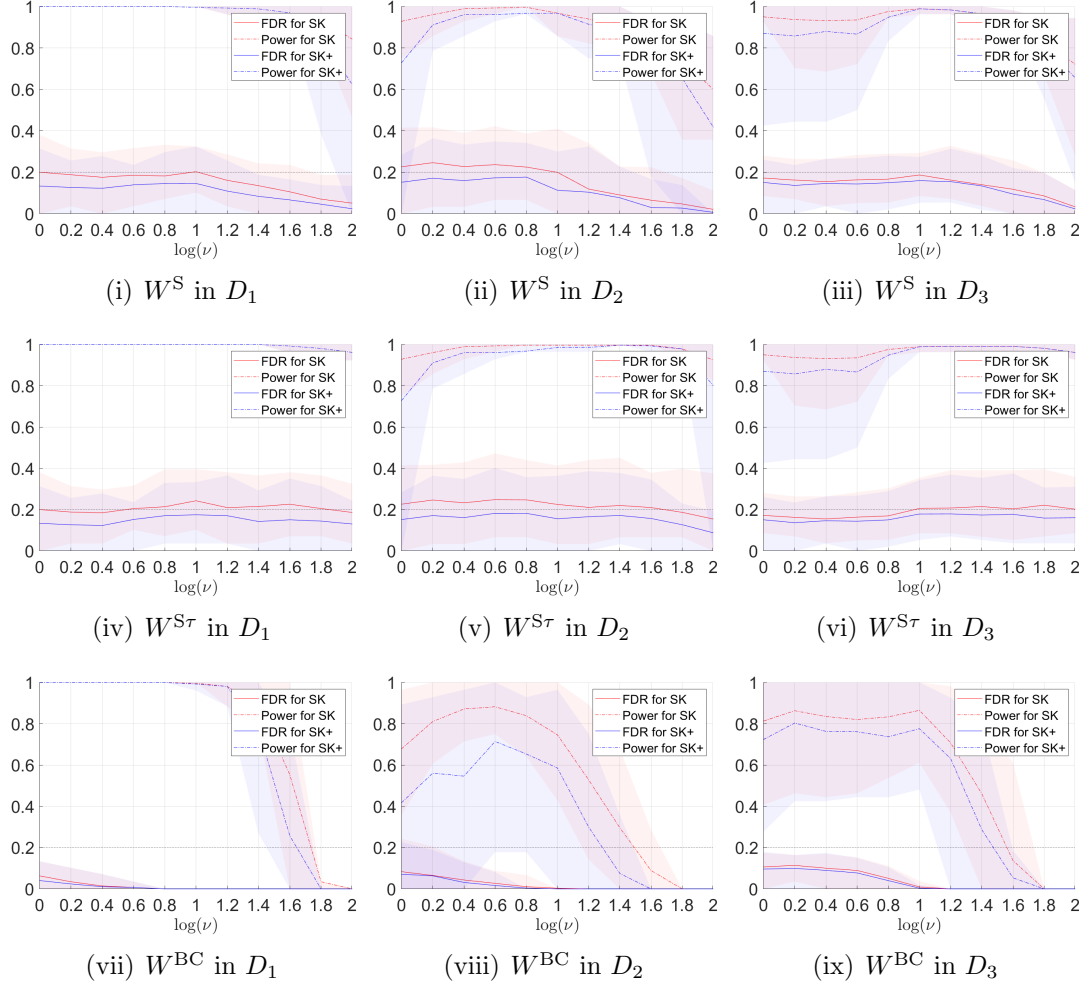


Figure 2: Performances of Split Knockoffs: FDR and Power for $q = 0.2$. $\beta(\lambda)$ is taken as $\beta_\nu(\lambda)$, the solution path of $\beta(\lambda)$ in the ν -Split LASSO path. The curves in the figures represent the average performances of Split Knockoffs in FDR and Power in 20 simulation instances, while the shaded areas represent the 80% confidence intervals.

$\beta(\lambda) = \hat{\beta}_{\hat{\nu}, \hat{\lambda}}$ achieve desired FDR in the family of W under all cases of transformational sparsity. In particular, Split Knockoffs with W^{BC} is more conservative than others with a lower FDR and the same power. In all cases, (Split) Knockoff+ has a better control in the FDR compared with (Split) Knockoff, at the cost of a potential loss in Power.

Compared with Knockoffs, Split Knockoffs exhibits higher power in the case of D_2 . In this case, the correlated X and D_2 destroys the incoherence condition of induced the LASSO problem (see Eq. (20) in Section 7.1 for discussions) such that Knockoffs suffer from losing the model selection consistency in the case of D_2 . It hurts the selection power for standard Knockoffs. In contrast, for Split Knockoffs, the improved ν -incoherence condition of Split LASSO as discussed in Section 4 leads to better path

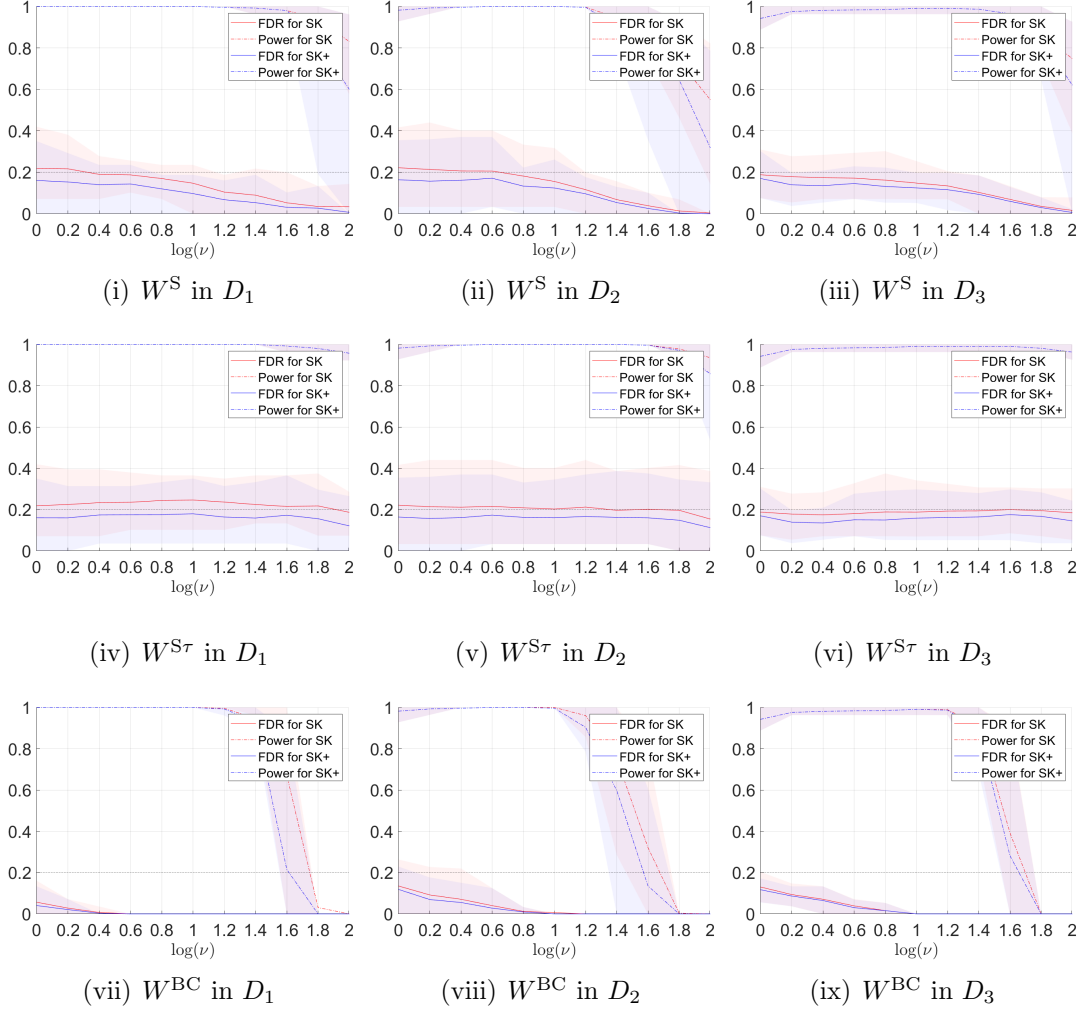


Figure 3: Performances of Split Knockoffs: FDR and Power for $q = 0.2$. $\beta(\lambda)$ is taken as a fixed cross validation optimal estimator $\hat{\beta}_{\hat{\nu}, \hat{\lambda}}$. The curves in the figures represent the average performances of Split Knockoffs in FDR and Power in 20 simulation instances, while the shaded areas represent the 80% confidence intervals.

consistency which helps improve the selection power.

6 Application: Alzheimer’s Disease

In this experiment, we apply the Split Knockoff method to study lesion regions of brains and their connections in Alzheimer’s Disease (AD), which is the major cause of dementia and attracts increasing attention in recent years.

Table 1: FDR and Power for Knockoffs and Split Knockoffs in simulation experiments ($q = 0.2$). The intercept $\beta(\lambda)$ for Split Knockoffs is taken as a fixed cross validation optimal estimator $\hat{\beta}_{\hat{\nu}, \hat{\lambda}}$, with the ν for calculating the feature and knockoff significance taken as $\hat{\nu}$. In this table, we present the average performances of Knockoffs and Split Knockoffs in FDR and Power, together with the standard deviations in 20 simulation instances. For shorthand notations, we use “SK(+)” to refer to “Split Knockoff(+)”.

Performances	Knockoff	SK with W^S	SK with $W^{S\tau}$	SK with W^{BC}
FDR in D_1	0.2413	0.2188	0.2188	0.0499
	± 0.1453	± 0.1436	± 0.1436	± 0.0655
Power in D_1	1.0000	1.0000	1.0000	1.0000
	± 0.0000	± 0.0000	± 0.0000	± 0.0000
FDR in D_2	0.2484	0.2152	0.2152	0.0822
	± 0.1798	± 0.1481	± 0.1481	± 0.0897
Power in D_2	0.4571	0.9893	0.9893	0.9893
	± 0.2917	± 0.0350	± 0.0350	± 0.0350
FDR in D_3	N/A	0.1872	0.1872	0.1200
	N/A	± 0.0928	± 0.0928	± 0.0608
Power in D_3	N/A	0.9519	0.9519	0.9519
	N/A	± 0.0435	± 0.0435	± 0.0435

Performances	Knockoff+	SK+ with W^S	SK+ with $W^{S\tau}$	SK+ with W^{BC}
FDR in D_1	0.1695	0.1605	0.1605	0.0339
	± 0.1560	± 0.1323	± 0.1323	± 0.0540
Power in D_1	1.0000	1.0000	1.0000	1.0000
	± 0.0000	± 0.0000	± 0.0000	± 0.0000
FDR in D_2	0.1072	0.1678	0.1678	0.0650
	± 0.1861	± 0.1351	± 0.1351	± 0.0874
Power in D_2	0.1750	0.9893	0.9893	0.9893
	± 0.3105	± 0.0350	± 0.0350	± 0.0350
FDR in D_3	N/A	0.1702	0.1702	0.1098
	N/A	± 0.0895	± 0.0895	± 0.0561
Power in D_3	N/A	0.9519	0.9519	0.9519
	N/A	± 0.0435	± 0.0435	± 0.0435

6.1 Dataset

The data is obtained from ADNI (<http://adni.loni.ucla.edu>) dataset, acquired by structural Magnetic Resonance Imaging (MRI) scan. In total, the dataset contains $n = 752$ samples, with 126 AD, 433 Mild Cognitive Impairment (MCI) and 193 Normal Controls (NC). For each image, we implement the Dartel VBM ([Ashburner, 2007](#))

for pre-processing, followed by the toolbox Statistical Parametric Mapping (SPM) for segmentation of gray matter (GM), white matter (WM) and cerebral spinal fluid (CSF). Then we use Automatic Anatomical Labeling (AAL) atlas (Tzourio-Mazoyer et al., 2002) to partition the whole brain into $p = 90$ Cerebrum brain anatomical regions, with the volume of each region (summation of all GMs in the region) provided.

We use $X \in \mathbb{R}^{n \times p}$ to denote the design matrix, with each element $X_{i,j}$ representing the column-wise normalized volume of region j in the subject i 's brain. The response variable vector $y \in \mathbb{R}^n$ denotes the Alzheimer's Disease Assessment Scale (ADAS), which was originally designed to assess the severity of cognitive dysfunction (Rosen et al., 1984) and was later found to be able to clinically distinguish the diagnosed AD from normal controls (Zec et al., 1992). We test two types of transformational sparsity:

- (a) $D = I_p$, the identity matrix, for selecting the regions that account for the Alzheimer's disease, where in this case $m = p = 90$;
- (b) D is the graph difference operator matrix on the brain region connectivity graph, for selecting the connections of regions with large activation changes accounting for the disease, where in this case $m = 463 > p = 90$;

In the analysis below, to maximize the selection power, the W statistics for Split Knockoff is taken to be $W^{S\tau}$, with $\beta(\lambda)$ being taken as a fixed cross validation optimal estimator $\hat{\beta}_{\hat{\nu}, \hat{\lambda}}$, screening on $\log \nu$ from a grid between 0 and 2 with a step size 0.4, and $\log \lambda$ from a grid between 0 and -8 with a step size 0.4. For the regularization paths in Eq. (7) and (9), we take $\log \lambda$ from an arithmetic sequence between 0 and -6 with step size $h_\lambda = 0.01$. In the experiments, We randomly split the dataset $\mathcal{D} = (X, y)$ into two parts $\mathcal{D}_1 = (X_1, y_1)$ and $\mathcal{D}_2 = (X_2, y_2)$ with n_1 and n_2 samples respectively where $n_1 = 150$ and $n_2 = n - n_1 = 702$. We show the experimental results on one random data split instance in this section, with the frequency plots on the most frequently selected regions and connections in multiple instances of data splits provided as supplementary materials in Section E.2.

6.2 Region Selection

In this experiment, we consider the selection of lesion regions, with $D = I_p$. We set our target FDR to be $q = 0.2$.

Our region selection results are summarized in Table 2 where $\log(\nu)$ is between 0 and 2 with a step size 0.1. At $\log \hat{\nu} = 0$ where $\hat{\beta}_{\hat{\nu}, \hat{\lambda}}$ is optimal in terms of cross validation loss, our algorithm selects five regions that are all related to AD and have been reported to suffer from degeneration during disease progression (Vemuri and Jack, 2010; Schuff et al., 2009; Karas et al., 2007; Greene et al., 2010). Specifically, it was reported in Vemuri and Jack (2010) that the hippocampus in both sides are responsible for learning and memory; while the middle temporal gyrus participates in language and memory processing. Moreover, Tyler et al. (2005) and Schremm et al. (2018) found that the opercular part of Inferior frontal gyrus may be associated with tone and inflectional

Table 2: Selected Regions by Split Knockoff on Alzheimer’s Disease ($q = 0.2$). The W statistics for Split Knockoff is taken to be $W^{S\tau}$, with $\beta(\lambda)$ taken as a fixed cross validation optimal estimator $\hat{\beta}_{\hat{\nu}, \hat{\lambda}}$, where the minimal cross validation loss lies on the choice $\log \hat{\nu} = 0$.

Region	Split Knockoff with $\log \nu$	
	[0, 1]	[1.1, 2]
Inferior frontal gyrus, opercular part (L)	✓	
Hippocampus (L)	✓	✓
Hippocampus (R)	✓	
Inferior parietal gyrus (R)	✓	
Middle temporal gyrus (L)	✓	

morpheme processing. Finally, the inferior parietal gyrus that is associated with motor and sensory, was found to suffer from volume reduction after the stage from normal control (NC) to mild cognitive impairment (Greene et al., 2010), *i.e.*, an intermediate stage between NC to Alzheimer’s Disease.

6.3 Connection Selection

In this experiment, we consider the connection or edge detection, in which each connection is associated with two adjacent brain regions. Formally speaking, we set D as the graph gradient (difference) operator on the graph $G = (V, E)$ where V denotes the vertex set of lesion regions and E denotes the (oriented) edge set of region pairs in neighbor, such that $D(\beta)(i, j) = \beta_i - \beta_j$ for $(i, j) \in E$. Thus D is the graph gradient operator that measures the difference in the impacts of Alzheimer’s Disease between adjacent regions in brains. We shall expect a properly selected edge will connect regions of high contrast variations in the degree of atrophy during the disease progression. For example, a selected edge may connect an atrophy region in the brain significantly impaired by Alzheimer’s Disease to another region which is less influenced by the disease.

For connection selection, our results are summarized in Table 3 where $\log(\nu)$ is between 0 and 2 with a step size 0.1. In total there are eleven connections being selected, six of which are selected at the cross-validation optimal $\hat{\nu}$. Among all the eleven selected connections, eight of them are associated with Hippocampus in the left side or the right side, where Hippocampus is one of the most early affected regions during disease progression (Juottonen et al., 1999). Similarly, the selected connections that involve Amygdala echo the previously findings that the Amygdala is also affected early (Knafo, 2012), which can explain the neuropsychiatric symptoms that are commonly observed in mild stages of AD. These studies provide us references of why these pairs of adjacent regions are with different degree of atrophy. Finally, the connection between Insula (L) and Middle frontal gyrus (L) may be a false discovery, as both regions were reported to be atrophied and this connection is not included in the cross-validation

Table 3: Selected connections by Split Knockoffs on Alzheimer’s Disease ($q = 0.2$). The W statistics for Split Knockoff is taken to be $W^{S\tau}$, with $\beta(\lambda)$ taken as a fixed cross validation optimal estimator $\hat{\beta}_{\hat{\nu}, \hat{\lambda}}$, where the minimal cross validation loss lies on the choice $\log \hat{\nu} = 0.4$.

Region 1	Connection	Region 2	Split Knockoff with $\log \nu$					
			[0, 0.1]	[0.2, 1.3]	1.4	1.5	[1.6, 1.7]	[1.8, 2]
Hippocampus (L)	Posterior cingulate gyrus (L)		✓	✓	✓			
Hippocampus (L)	Lingual gyrus (L)		✓	✓	✓	✓		
Hippocampus (L)	Fusiform gyrus (L)		✓					
Hippocampus (L)	Precuneus (L)		✓	✓	✓	✓	✓	
Hippocampus (R)	Insula (R)		✓					
Hippocampus (R)	Lingual gyrus (R)		✓	✓				
Hippocampus (R)	Precuneus (R)		✓	✓				
Hippocampus (R)	Superior temporal gyrus (R)		✓					
Amygdala (R)	Putamen (R)		✓		✓			
Amygdala (R)	Caudate nucleus (R)		✓					
Middle frontal gyrus, orbital part (L)	Insula (L)		✓					

optimal selection. Although it was found that the atrophy happens in the whole region of Insula while only sub-region of middle frontal gyrus (Busatto et al., 2008), it is still ambiguous to claim that the involved regions are significantly different in terms of degrees of degeneration. In summary, the selected regions and connections at cross-validation optimal $\hat{\nu}$ are illustrated in Figure 1.

7 Discussion

In this section, we first discuss a straightforward way of conducting Knockoffs on generalized LASSO under special cases of transformational sparsity, and why such a procedure does not work in general. Then we discuss how the exchangeability property fails for Split Knockoffs and the challenges for provable FDR control.

7.1 Generalized LASSO and Knockoffs

Within the large literature dealing with the transformational sparsity problem, generalized LASSO (Tibshirani et al., 2011) is the most popular way to handle such problem. In some special cases, it can be converted to sparse linear regression where one can design knockoffs; yet in general, it is open how to do so.

Recall that the generalized LASSO solves the optimization problem below with $\lambda > 0$,

$$\min_{\beta} \frac{1}{2n} \|y - X\beta\|_2^2 + \lambda \|D\beta\|_1. \quad (19)$$

Particularly, if $\text{rank } D = m \leq p$, this problem can be equivalently represented by the following LASSO procedure with respect to $\lambda > 0$,

$$\min_{\gamma} \frac{1}{2n} \|y - XD^\dagger\gamma - XD_0\gamma_0\|_2^2 + \lambda \|\gamma\|_1,$$

where $D^\dagger \in \mathbb{R}^{p \times m}$ is the pseudo inverse for D , $D_0 \in \mathbb{R}^{p \times (p - \text{rank } D)}$ is a matrix whose columns spans the $\ker(D)$, and $\gamma_0 \in \mathbb{R}^{p - \text{rank } D}$ is the representation coefficient for the null space $\ker(D)$ without sparsity. Note that we can write $\beta^* = D^\dagger \gamma^* + D_0 \gamma_0^*$ for some $\gamma_0^* \in \mathbb{R}^{p - \text{rank } D}$, and Equation (1) becomes simply

$$y = XD^\dagger \gamma^* + XD_0 \gamma_0^* + \varepsilon.$$

In this special case of $\text{rank } D = m \leq p$, one can construct knockoffs like standard sparse linear regression. To see this, Take $U \in \mathbb{R}^{n \times (n - p + \text{rank } D)}$ as an orthogonal complement for the column space of $XD_0 \in \mathbb{R}^{n \times (p - \text{rank } D)}$, we have

$$U^T y = U^T XD^\dagger \gamma^* + U^T \varepsilon. \quad (20)$$

We can treat $U^T XD^\dagger$ as a new design matrix, $U^T y$ as the response vector and $U^T \varepsilon \sim \mathcal{N}(0, I_{n-p+\text{rank } D})$ as the Gaussian noise. Then the problem is transferred to a sparse linear regression problem and we can apply the standard knockoff method with FDR control.

However, a shortcoming of this approach may suffer the poor power when D is nontrivial and/or X is highly co-related, such that the incoherence requirements for sparse recovery or model selection consistency (Donoho and Huo, 2001; Tropp, 2004; Zhao and Yu, 2006; Wainwright, 2009; Osher et al., 2016; Huang et al., 2020) fail for the design matrix $U^T XD^\dagger$.

Furthermore, this conversion does not work in the setting $m > p$. If $m > p$, γ lies in the column space of D , a proper subspace of \mathbb{R}^m , and it remains open how to design a knockoff method under such a constraint.

7.2 Failure of Exchangeability in Split Knockoffs

The main challenge in establishing the FDR control of Split Knockoffs lies in the failure of exchangeability. In this section, we provide the details on how the exchangeability property of classical Knockoffs fails in Split Knockoffs.

Specifically, Barber et al. (2015) (Lemma 2-3), established pairwise exchangeability for both features and responses in standard knockoffs, the latter of which however fails in Split Knockoffs.

Proposition 7.1 (Failure of Pairwise Exchangeability). *For any $S \subseteq S_0$, there holds*

$$[A_\gamma, \tilde{A}_\gamma]_{\text{swap}\{S\}}^T [A_\gamma, \tilde{A}_\gamma]_{\text{swap}\{S\}} = [A_\gamma, \tilde{A}_\gamma]^T [A_\gamma, \tilde{A}_\gamma], \quad (21a)$$

$$[A_\gamma, \tilde{A}_\gamma]_{\text{swap}\{S\}}^T \tilde{y} \stackrel{d}{\neq} [A_\gamma, \tilde{A}_\gamma]^T \tilde{y}, \quad (21b)$$

where $[A_\gamma, \tilde{A}_\gamma]_{\text{swap}\{S\}}$ denotes a swap of the j -th column of A_γ and \tilde{A}_γ in $[A_\gamma, \tilde{A}_\gamma]$ for $j \in S$.

In other words, for Split Knockoffs, while pairwise exchangeability for features holds in (21a), that for responses fails in (21b). To see the details for Proposition 7.1, we first calculate that

$$A_\gamma^T \tilde{y} = 0, \quad \tilde{A}_\gamma^T \tilde{y} = \frac{\tilde{A}_{\gamma,1}^T}{\sqrt{n_2}} X_2 \beta^* + \frac{\tilde{A}_{\gamma,1}^T}{\sqrt{n}} \varepsilon_2, \quad (22)$$

where $\tilde{A}_\gamma = [\tilde{A}_{\gamma,1}^T, \tilde{A}_{\gamma,2}^T]^T$ with $\tilde{A}_{\gamma,1}^T \in \mathbb{R}^{n_2 \times m}$ and $\tilde{A}_{\gamma,2}^T \in \mathbb{R}^{m \times m}$. Recall that from (6), there holds

$$\tilde{A}_{\gamma,1}^T \frac{X_2}{\sqrt{n_2}} + \tilde{A}_{\gamma,2}^T \frac{D}{\sqrt{\nu}} = -\frac{D}{\nu}, \quad -\frac{\tilde{A}_{\gamma,2}^T}{\sqrt{\nu}} = \frac{I}{\nu} - \text{diag}\{s\}. \quad (23)$$

Then there holds $\tilde{A}_{\gamma,1}^T \frac{X_2}{\sqrt{n_2}} = \text{diag}\{s\} D$. Combining it with Equation (22), there holds

$$[A_\gamma, \tilde{A}_\gamma]^T \tilde{y} = \begin{bmatrix} 0 \\ -\text{diag}\{s\} \gamma^* + \frac{\tilde{A}_{\gamma,1}^T}{\sqrt{n}} \varepsilon \end{bmatrix}. \quad (24)$$

Then the distribution of $[A_\gamma, \tilde{A}_\gamma]^T \tilde{y}$ is normal

$$\mathcal{N} \left(\begin{bmatrix} 0 \\ -\text{diag}\{s\} \gamma^* \end{bmatrix}, \begin{bmatrix} 0 & 0 \\ 0 & \frac{\sigma^2}{n_2} \tilde{A}_{\gamma,1}^T \tilde{A}_{\gamma,1} \end{bmatrix} \right), \quad (25)$$

where swapping any $i \in S_0$ in the second and the third block will lead to different Normal distributions of different covariance matrices.

The failure of exchangeability may impose a theoretical challenge for knockoff based methods, as the beautiful symmetry results (Barber et al., 2015) can not be applicable. For random designs, Barber et al. (2020) exploits KL divergence to measure the “distance” to exchangeability, and then gives approximate but not exact FDR control based on the “distance”. It is also worth to mention that this method no longer relies on the martingale arguments and use direct analysis. However, it is not clear how to apply such methods to fixed designs in our scenario. Instead, our strategy in this paper is to exploit the orthogonal design in Split Lasso and the data splitting that leave us independent signs of Split Knockoff statistics, recovering an inverse supermartingale structure like Barber et al. (2019) without using the exchangeability.

8 Conclusion

In this paper, we propose Split Knockoffs as a data adaptive FDR control method for the transformational sparsity recovery in linear regression where a linear transformation of parameters is sparse. By relaxing the linear subspace constraint to its neighborhood in a lifted parameter space, our method has FDR under control and further gains power in improving the model selection consistency conditions on Split LASSO regularization

paths. The main theoretical contribution of this paper is that we construct some new supermartingale structure to give a theoretical FDR control for Split Knockoffs where exchangeability is broken by the heterogeneous noise. In a real world application to Alzheimer’s Disease study with MRI data, Split Knockoffs discover important atrophy lesion regions in brain and neighboring region connections of high contrast in atrophy variations during disease progression. Future directions include generalizations of our methodology to random designs.

References

J. Ashburner. A fast diffeomorphic image registration algorithm. *Neuroimage*, 38(1):95–113, 2007.

R. F. Barber, E. J. Candès, et al. Controlling the false discovery rate via knockoffs. *The Annals of Statistics*, 43(5):2055–2085, 2015.

R. F. Barber, E. J. Candès, et al. A knockoff filter for high-dimensional selective inference. *Annals of Statistics*, 47(5):2504–2537, 2019.

R. F. Barber, E. J. Candès, R. J. Samworth, et al. Robust inference with knockoffs. *Annals of Statistics*, 48(3):1409–1431, 2020.

Y. Benjamini and Y. Hochberg. Controlling the false discovery rate: a practical and powerful approach to multiple testing. *Journal of the Royal Statistical Society: series B (Methodological)*, 57(1):289–300, 1995.

G. F. Busatto, B. S. Diniz, and M. V. Zanetti. Voxel-based morphometry in Alzheimer’s disease. *Expert review of neurotherapeutics*, 8(11):1691–1702, 2008.

J.-F. Cai, B. Dong, S. Osher, and Z. Shen. Image restoration: Total variation, wavelet frames, and beyond. *J. Amer. Math. Soc.*, 25(4):1033–1089, 2012.

E. Candès, Y. Fan, L. Janson, and J. Lv. Panning for gold: Model-X knockoffs for high-dimensional controlled variable selection. *Journal of the Royal Statistical Society: series B (Statistical Methodology)*, 80(3):551–577, 2018.

R. Dai and R. F. Barber. The knockoff filter for FDR control in group-sparse and multitask regression. In *Proceedings of The 33rd International Conference on Machine Learning (ICML)*, 2016. PMLR 48:1851–1859. arXiv:1602.03589.

D. L. Donoho and X. Huo. Uncertainty principles and ideal atomic decomposition. *IEEE Transactions on Information Theory*, 47(7):2845–2862, 2001.

D. L. Donoho and I. M. Johnstone. Adapting to unknown smoothness via wavelet shrinkage. *Journal of the American Statistical Association*, 90(432):1200–1224, 1995.

J. Friedman, T. Hastie, and R. Tibshirani. Regularization paths for generalized linear models via coordinate descent. *Journal of statistical software*, 33(1):1, 2010.

S. J. Greene, R. J. Killiany, Alzheimer’s Disease Neuroimaging Initiative, et al. Sub-regions of the inferior parietal lobule are affected in the progression to Alzheimer’s disease. *Neurobiology of aging*, 31(8):1304–1311, 2010.

C. Huang, X. Sun, J. Xiong, and Y. Yao. Split LBI: An iterative regularization path with structural sparsity. In *Advances in Neural Information Processing Systems (NIPS) 29*, pages 3369–3377. 2016.

C. Huang, X. Sun, J. Xiong, and Y. Yao. Boosting with structural sparsity: A differential inclusion approach. *Applied and Computational Harmonic Analysis*, 48(1):1–45, 2020.

K. Juottonen, M. P. Laakso, K. Partanen, and H. Soininen. Comparative MR analysis of the entorhinal cortex and hippocampus in diagnosing Alzheimer disease. *American Journal of Neuroradiology*, 20(1):139–144, 1999.

G. Karas, P. Scheltens, S. Rombouts, R. Van Schijndel, M. Klein, B. Jones, W. Van Der Flier, H. Vrenken, and F. Barkhof. Precuneus atrophy in early-onset Alzheimer’s disease: a morphometric structural MRI study. *Neuroradiology*, 49(12):967–976, 2007.

S.-J. Kim, K. Koh, S. Boyd, and D. Gorinevsky. ℓ_1 trend filtering. *SIAM review*, 51(2):339–360, 2009.

S. Knafo. Amygdala in Alzheimer’s disease. *The Amygdala—A Discrete Multitasking Manager*. IntechOpen, pages 375–383, 2012.

S. Osher, F. Ruan, J. Xiong, Y. Yao, and W. Yin. Sparse recovery via differential inclusions. *Applied and Computational Harmonic Analysis*, 41(2):436–469, 2016.

Z. Ren and E. Candès. Knockoffs with side information. 2020.

Z. Ren, Y. Wei, and E. Candès. Derandomizing knockoffs. *Journal of American Statistical Association*, 2021.

Y. Romano, M. Sesia, and E. Candès. Deep knockoffs. *Journal of the American Statistical Association*, pages 1–12, 2019.

W. G. Rosen, R. C. Mohs, and K. L. Davis. A new rating scale for Alzheimer’s disease. *Am J Psychiatry*, 141(11):1356–64, 1984.

L. I. Rudin, S. Osher, and E. Fatemi. Nonlinear total variation based noise removal algorithms. *Physica D: Nonlinear Phenomena*, 60(1-4):259–268, 1992.

A. Schremm, M. Novén, M. Horne, P. Söderström, D. van Westen, and M. Roll. Cortical thickness of planum temporale and pars opercularis in native language tone processing. *Brain and Language*, 176:42–47, 2018.

N. Schuff, N. Woerner, L. Boreta, T. Kornfield, L. Shaw, J. Trojanowski, P. Thompson, C. Jack Jr, M. Weiner, and A. D. N. Initiative. MRI of hippocampal volume loss in early Alzheimer’s disease in relation to apoe genotype and biomarkers. *Brain*, 132(4):1067–1077, 2009.

N. Simon, J. Friedman, T. Hastie, and R. Tibshirani. Regularization paths for cox’s proportional hazards model via coordinate descent. *Journal of statistical software*, 39(5):1, 2011.

R. Tibshirani, M. Saunders, S. Rosset, J. Zhu, and K. Knight. Sparsity and smoothness via the fused lasso. *Journal of the Royal Statistical Society: Series B (Statistical Methodology)*, 67(1):91–108, 2005.

R. J. Tibshirani, J. Taylor, et al. The solution path of the generalized lasso. *The Annals of Statistics*, 39(3):1335–1371, 2011.

J. A. Tropp. Greed is good: Algorithmic results for sparse approximation. *IEEE Trans. Inform. Theory*, 50(10):2231–2242, 2004.

L. K. Tyler, E. A. Stamatakis, B. Post, B. Randall, and W. Marslen-Wilson. Temporal and frontal systems in speech comprehension: An fMRI study of past tense processing. *Neuropsychologia*, 43(13):1963–1974, 2005.

N. Tzourio-Mazoyer, B. Landeau, D. Papathanassiou, F. Crivello, O. Etard, N. Delcroix, B. Mazoyer, and M. Joliot. Automated anatomical labeling of activations in SPM using a macroscopic anatomical parcellation of the MNI MRI single-subject brain. *Neuroimage*, 15(1):273–289, 2002.

P. Vemuri and C. R. Jack. Role of structural MRI in Alzheimer’s disease. *Alzheimer’s research & therapy*, 2(4):1–10, 2010.

M. J. Wainwright. Sharp thresholds for high-dimensional and noisy sparsity recovery using l_1 -constrained quadratic programming (LASSO). *IEEE Transactions on Information Theory*, 55(5):2183–2202, 2009.

Q. Xu, J. Xiong, X. Cao, and Y. Yao. False discovery rate control and statistical quality assessment of annotators in crowdsourced ranking. In *International Conference on Machine Learning*, pages 1282–1291, 2016.

R. F. Zec, E. S. Landreth, S. K. Vicari, E. Feldman, J. Belman, A. Andrise, R. Robbs, V. Kumar, and R. Becker. Alzheimer disease assessment scale: useful for both early detection and staging of dementia of the Alzheimer type. *Alzheimer Disease and Associated Disorders*, 1992.

P. Zhao and B. Yu. On model selection consistency of Lasso. Journal of Machine learning research, 7(Nov):2541–2563, 2006.

SUPPLEMENTARY MATERIAL

A Construction of Split Knockoff Copies

In this section, we provide more details on the construction of Split Knockoff copy matrices. An explicit form of such constructions is shown in the following proposition.

Proposition A.1 (Split Knockoff Matrix). *For any vector s in Equation (6) satisfying*

$$\text{diag}(s) \succeq 0, \quad 2C_\nu - \text{diag}(s) \succeq 0, \quad (26)$$

where $C_\nu := \Sigma_{\gamma,\gamma} - \Sigma_{\gamma,\beta}\Sigma_{\beta,\beta}^\dagger\Sigma_{\beta,\gamma}$, $\Sigma_{\beta,\beta} := A_\beta^T A_\beta$, $\Sigma_{\beta,\gamma} = \Sigma_{\gamma,\beta}^T := A_\beta^T A_\gamma$, and $\Sigma_{\gamma,\gamma} := A_\gamma^T A_\gamma$, there is a valid Split Knockoff matrix for $n_2 \geq m + p$,

$$\tilde{A}_\gamma = A_\gamma(I_m - C_\nu^{-1}\text{diag}(s)) + A_\beta\Sigma_{\beta,\beta}^{-1}\Sigma_{\beta,\gamma}C_\nu^{-1}\text{diag}(s) + \tilde{U}K, \quad (27)$$

where $\tilde{U} \in \mathbb{R}^{(n_2+m) \times m}$ is the orthogonal complement of $[A_\beta, A_\gamma]$ and $K \in \mathbb{R}^{m \times m}$ satisfies $K^T K = 2\text{diag}(s) - \text{diag}(s)C_\nu^{-1}\text{diag}(s)$.

Since $\tilde{U} \in \mathbb{R}^{(n_2+m) \times m}$ here is an orthogonal complement of $[A_\beta, A_\gamma] \in \mathbb{R}^{(n_2+m) \times (m+p)}$, it requires $n_2 \geq m + p$. Next, we will show that any s satisfying Eq. (26) will ensure the existence of \tilde{A}_γ .

Note that a necessary and sufficient condition for the existence of \tilde{A}_γ satisfying Equation (6) is

$$G := \begin{bmatrix} \Sigma_{\beta,\beta} & \Sigma_{\beta,\gamma} & \Sigma_{\beta,\gamma} \\ \Sigma_{\beta,\gamma} & \Sigma_{\gamma,\gamma} & \Sigma_{\gamma,\gamma} - \text{diag}(s) \\ \Sigma_{\beta,\gamma} & \Sigma_{\gamma,\gamma} - \text{diag}(s) & \Sigma_{\gamma,\gamma} \end{bmatrix} \succeq 0.$$

This holds if and only if the Schur complement of $\Sigma_{\beta,\beta}$ is positive semi-definite, i.e.

$$\begin{bmatrix} C_\nu & C_\nu - \text{diag}(s) \\ C_\nu - \text{diag}(s) & C_\nu \end{bmatrix} \succeq 0, \quad C_\nu := \Sigma_{\gamma,\gamma} - \Sigma_{\gamma,\beta}\Sigma_{\beta,\beta}^\dagger\Sigma_{\beta,\gamma},$$

which holds if and only if C_ν and its Schur complement are positive semi-definite, i.e.

$$\begin{aligned} C_\nu &\succeq 0, \\ C_\nu - (C_\nu - \text{diag}(s))C_\nu^{-1}(C_\nu - \text{diag}(s)) &= 2\text{diag}(s) - \text{diag}(s)C_\nu^{-1}\text{diag}(s) \succeq 0. \end{aligned}$$

It is equivalent to Equation (26). Then one can verify that the construction in Proposition A.1 satisfies Equation (6) with the vector s satisfying Eq. (26).

There are various choices for $s = (s_i)$ satisfying (26) for Split Knockoffs. Below we give two typical examples.

(a) (SDP for discrepancy maximization) One can maximize the discrepancy between Knockoffs and its corresponding features by solving the following SDP

$$\begin{aligned} & \text{maximize} && \sum_i s_i, \\ & \text{subject to} && 0 \leq s_i \leq \frac{1}{\nu}, \\ & && \frac{\text{diag}(s)}{2} \preceq A_\gamma^T (I - H) A_\gamma, \end{aligned}$$

where

$$H = A_\beta (A_\beta^T A_\beta)^{-1} A_\beta^T = \begin{bmatrix} \frac{X_2}{\sqrt{n_2}} \\ \frac{D}{\sqrt{\nu}} \end{bmatrix} \left[\frac{X_2^T X_2}{n_2} + \frac{D^T D}{\nu} \right]^{-1} \begin{bmatrix} X_2^T \\ \frac{D^T}{\sqrt{n_2}} \end{bmatrix},$$

and

$$A_\gamma^T (I - H) A_\gamma = A_\gamma^T A_\gamma - A_\gamma^T H A_\gamma = \frac{I}{\nu} - \frac{D}{\nu} \left[\frac{X_2^T X_2}{n_2} + \frac{D^T D}{\nu} \right]^{-1} \frac{D^T}{\nu} = C_\nu.$$

(b) (Equi-correlation) Take $s_i = 2\lambda_{\min}(C_\nu) \wedge \frac{1}{\nu}$ for all $i \in \{1, 2, \dots, m\}$. Then we have,

$$A_\gamma^T \tilde{A}_\gamma = \left[\frac{1}{\nu} - 2\lambda_{\min}(C_\nu) \wedge \frac{1}{\nu} \right] I_m.$$

B Proof for Theorem 3.1

In this section, we will give a complete proof for Theorem 3.1. Our treatment includes the following four types of W -statistics:

1. $W^S := Z \odot \text{sign}(Z - \tilde{Z})$, where S refers to ‘‘Split’’.
2. $W^{S\tau} := Z \odot \text{sign}(Z - \tau(\tilde{Z}))$, where $S\tau$ refers to applying truncation (11) on W^S .
3. $W^{BC} := (Z \vee \tilde{Z}) \odot \text{sign}(Z - \tilde{Z})$, where BC refers to the original definition adopted by Barber-Candès in Barber et al. (2015).
4. $W^{BC\tau} := (Z \vee \tau(\tilde{Z})) \odot \text{sign}(Z - \tau(\tilde{Z}))$, where $BC\tau$ refers to applying truncation (11) on W^{BC} .

The last one $W^{BC\tau}$ is added here for completeness. For shorthand notation, we use W^* to represent any one of the four cases, where $\star \in \{S, S\tau, BC, BC\tau\}$, as well as by $(S\star, BC\star)$ denote one of the pairs in $\{(S, BC), (S\tau, BC\tau)\}$ with truncation τ adopted or not.

We will first show that by a standard procedure in Knockoffs as in [Barber et al. \(2015\)](#), the problem of bounding the FDR by q can be transferred into the problem of bounding $\mathbb{E} [\mathcal{M}_{T_q^*}(W^*)]$ by one, where

$$\mathcal{M}_T(W^*) = \frac{\sum_{i \in S_0} 1\{W_i^* \geq T\}}{1 + \sum_{i \in S_0} 1\{W_i^* \leq -T\}}. \quad (29)$$

Following that, we divide the proof into two parts:

1. In Section [B.1](#), we will prove that $\mathbb{E} [\mathcal{M}_{T_q^{S*}}(W^{S*})] \leq 1$ by introducing an inverse supermartingale structure associated with $\mathcal{M}_T(W^{S*})$.
2. In Section [B.2](#), We will show that T_q^{BC*} is a stopping time with respect to a filtration associated with $\mathcal{M}_T(W^{S*})$, which enables us to show that $\mathbb{E} [\mathcal{M}_{T_q^{BC*}}(W^{BC*})] \leq \mathbb{E} [\mathcal{M}_{T_q^{BC*}}(W^{S*})] \leq 1$.

We begin the proof from the following common procedure of Knockoffs ([Barber et al., 2015](#)), that the upper bound of FDR in the case of W^* is transferred into the upper bound of $\mathbb{E} [\mathcal{M}_{T_q^*}(W^*)]$. The procedure goes as the following for Split Knockoff(+).

(a) (Split Knockoff) The modified FDR can be bounded by the following product:

$$\mathbb{E} \left[\frac{\sum_{i \in S_0} 1\{W_i^* \geq T_q^*\}}{\sum_i 1\{W_i^* \geq T_q^*\} + q^{-1}} \right] \leq \mathbb{E} \left[\frac{1 + \sum_i 1\{W_i^* \leq -T_q^*\}}{\sum_i 1\{W_i^* \geq T_q^*\} + q^{-1}} \frac{\sum_{i \in S_0} 1\{W_i^* \geq T_q^*\}}{1 + \sum_{i \in S_0} 1\{W_i^* \leq -T_q^*\}} \right]. \quad (30)$$

By the definition of the Split Knockoff threshold, there holds

$$\frac{\sum_i 1\{W_i^* \leq -T_q^*\}}{1 \vee \sum_i 1\{W_i^* \geq T_q^*\}} \leq q \leq 1,$$

which implies

$$\sum_i 1\{W_i^* \leq -T_q^*\} \leq q \sum_i 1\{W_i^* \geq T_q^*\}.$$

Consequently, there holds

$$\frac{1 + \sum_i 1\{W_i^* \leq -T_q^*\}}{\sum_i 1\{W_i^* \geq T_q^*\} + q^{-1}} \leq \frac{1 + q[\sum_i 1\{W_i^* \geq T_q^*\}]}{\sum_i 1\{W_i^* \geq T_q^*\} + q^{-1}} = q.$$

Combined with Equation (30), there holds

$$\mathbb{E} \left[\frac{\sum_{i \in S_0} 1\{W_i^* \geq T_q^*\}}{\sum_i 1\{W_i^* \geq T_q^*\} + q^{-1}} \right] \leq q \mathbb{E} \left[\frac{\sum_{i \in S_0} 1\{W_i^* \geq T_q^*\}}{1 + \sum_{i \in S_0} 1\{W_i^* \leq -T_q^*\}} \right] = q \mathbb{E} [\mathcal{M}_{T_q^*}(W^*)]. \quad (31)$$

(b) (Split Knockoff+) The following lines established the result,

$$\begin{aligned}
\mathbb{E} \left[\frac{\sum_{i \in S_0} 1\{W_i^* \geq T_q^*\}}{1 \vee \sum_i 1\{W_i^* \geq T_q^*\}} \right] &\leq \mathbb{E} \left[\frac{1 + \sum_i 1\{W_i^* \leq -T_q^*\}}{1 \vee \sum_i 1\{W_i^* \geq T_q^*\}} \frac{\sum_{i \in S_0} 1\{W_i^* \geq T_q^*\}}{1 + \sum_{i \in S_0} 1\{W_i^* \leq -T_q^*\}} \right], \\
&\leq q \mathbb{E} \left[\frac{\sum_{i \in S_0} 1\{W_i^* \geq T_q^*\}}{1 + \sum_{i \in S_0} 1\{W_i^* \leq -T_q^*\}} \right] = q \mathbb{E} [\mathcal{M}_{T_q^*}(W^*)].
\end{aligned} \tag{32}$$

Then we transfer the problem of bounding FDR by q in Theorem 3.1 into the problem of bounding $\mathbb{E} [\mathcal{M}_{T_q^*}(W^*)]$ by one using Eq. (31) and Eq. (32). Then we will prove the following two inequalities respectively in Section B.1 and Section B.2.

1. We will first prove that $\mathbb{E} [\mathcal{M}_{T_q^*}(W^{S*})] \leq 1$ in Section B.1.
2. We will then show that $\mathbb{E} [\mathcal{M}_{T_q^{BC*}}(W^{BC*})] \leq \mathbb{E} [\mathcal{M}_{T_q^*}(W^{S*})] \leq 1$ in Section B.2.

B.1 Proof for Theorem 3.1: Case I

As a reminder for the notations, S^* is an arbitrary element from $(S, S\tau)$. We show in this part that Theorem 3.1 holds in the case of W^{S*} . In this section, We will target to formulate a supermartingale structure associated with $\mathcal{M}_T(W^{S*})$. In order to do such a thing, we will need to show that W^{S*} is a statistics whose sign ($\text{sign}(W^{S*})$) and length ($|W^{S*}|$) are independent from each other.

To show such a independence property, we will need to take a deeper look at the KKT conditions of Eq. (7) and Eq. (9). From Eq. (7) and Eq. (9), the KKT conditions that the solution $\gamma(\lambda)$, $\tilde{\gamma}(\lambda)$ with respect to $\lambda > 0$ should satisfy is

$$\lambda \rho(\lambda) + \frac{\gamma(\lambda)}{\nu} = \frac{D\beta(\lambda)}{\nu}, \tag{33a}$$

$$\lambda \tilde{\rho}(\lambda) + \frac{\tilde{\gamma}(\lambda)}{\nu} = \frac{D\beta(\lambda)}{\nu} + \underbrace{\left\{ -\text{diag}(s)\gamma^* + \frac{\tilde{A}_{\gamma,1}^T \varepsilon_2}{\sqrt{n_2}} \right\}}_{=:\zeta}, \tag{33b}$$

where $\rho(\lambda) \in \partial\|\gamma(\lambda)\|_1$, $\tilde{\rho}(\lambda) \in \partial\|\tilde{\gamma}(\lambda)\|_1$, and $\tilde{A}_{\gamma,1} \in \mathbb{R}^{n_2 \times m}$ is defined to be the submatrix of \tilde{A}_γ as the first n_2 rows. The details on the calculation of the term $A_\gamma^T \tilde{y}$ can be found in Eq. (40), while the other terms can be calculated directly following the definitions. For shorthand notations, we denote $\zeta := -\text{diag}(s)\gamma^* + \frac{\tilde{A}_{\gamma,1}^T \varepsilon_2}{\sqrt{n_2}}$.

Then from the definition, there holds

1. $\beta(\lambda)$ from $\mathcal{D}_1 = (X_1, y_1)$ and ζ from $\mathcal{D}_2 = (X_2, y_2)$ are independent from each other;

2. $\gamma(\lambda)$ is determined by $\beta(\lambda)$ from $\mathcal{D}_1 = (X_1, y_1)$, so is Z and $r := \text{sign}(\gamma(Z-))$ as functions of $\gamma(\lambda)$;
3. conditional on $\beta(\lambda)$, $\tilde{\gamma}$ is determined by ζ from $\mathcal{D}_2 = (X_2, y_2)$, so is \tilde{Z} , $\tilde{r} := \text{sign}(\tilde{\gamma}(\tilde{Z}-))$, and $\tau(\tilde{Z})$ as functions of $\tilde{\gamma}$.

Therefore, conditional on $\beta(\lambda)$ from $\mathcal{D}_1 = (X_1, y_1)$ which determines $|W^{S^*}| = Z$, the difference between the feature significance (33a) and knockoff significance (33b) lies on the random variable ζ from $\mathcal{D}_2 = (X_2, y_2)$. Thus the length $|W^{S^*}|$ and sign $\{\text{sign}(W^{S^*})\}$ of W^{S^*} are independent from each other. Additional calculations on ζ shows that ζ are consist of independent Gaussian random variables, i.e. for the Split Knockoff matrix satisfying (6),

$$\zeta \sim \mathcal{N} \left(-\text{diag}(s)\gamma^*, \frac{1}{n_2} \text{diag}(s)(2I_m - \text{diag}(s)\nu)\sigma^2 \right),$$

where the details can be found in Eq. (42) in Section C. Then we can give the following lemma.

Lemma B.1 (Lemma 3.2). *Given any determined $\beta(\lambda)$, $|W^{S^*}| = Z$ are determined, with $\text{sign}(W^{S^*})$ determined by ζ . Then $1\{W_i^{S^*} < 0\}$ are some independent Bernoulli random variables. Furthermore, for $i \in S_0$, there holds*

$$\mathbb{P}[1\{W_i^{S^*} < 0\} = 1] \geq \frac{1}{2}.$$

In particular, there holds $\mathbb{P}[1\{W_i^{S^*} < 0\} = 1] = \frac{1}{2}$ for $i \in S_0$. Moreover, the set $\{\exists i : W_i^{S^*} = 0\}$ will be of measure zero, and will be excluded from further discussions for convenience.

For shorthand notations, we rearrange the index on of W^{S^*} , such that $|W_{(1)}^{S^*}| \geq |W_{(2)}^{S^*}| \geq \dots \geq |W_{(m^*)}^{S^*}|$, and $\{(1), (2), \dots, (m^*)\} = S_0$, where $m^* = |S_0| \leq m$. Further denote $B_{(i)} = 1\{W_{(i)}^{S^*} < 0\}$, then there holds

$$\begin{aligned} \frac{\sum_{i \in S_0} 1\{W_i^{S^*} \geq T_q^{S^*}\}}{1 + \sum_{i \in S_0} 1\{W_i^{S^*} \leq -T_q^{S^*}\}} &= \frac{1 + \sum_{i \in S_0} 1\{|W_i^{S^*}| \geq T_q^{S^*}\}}{1 + \sum_{i \in S_0} 1\{|W_i^{S^*}| \geq T_q^{S^*}, W_i^{S^*} < 0\}} - 1, \\ &= \frac{1 + J}{1 + B_{(1)} + B_{(2)} + \dots + B_{(J)}} - 1, \end{aligned} \tag{34}$$

where $J \leq m^*$ is defined to be the index satisfying

$$|W_{(1)}^{S^*}| \geq |W_{(2)}^{S^*}| \geq \dots \geq |W_{(J)}^{S^*}| \geq T_q^{S^*} > |W_{(J+1)}^{S^*}| \geq \dots \geq |W_{(m^*)}^{S^*}|,$$

in other words, $J = \text{argmax}_{k \leq m^*} \{|W_{(k)}^{S^*}| \geq T_q^{S^*}\}$.

Define the filtration $\{\mathcal{F}_j\}_{j=1}^m$ and $\{\mathcal{G}_j\}_{j=1}^m$ in inverse time as

$$\mathcal{F}_j = \sigma \left(\left\{ \sum_{i=1}^j B_{(i)}, \zeta_{(j+1)}, \dots, \zeta_{(m)} \right\} \right),$$

$$\mathcal{G}_j = \sigma \left(\left\{ \sum_{i=1}^j B_{(i)}, B_{(j+1)}, \dots, B_{(m)} \right\} \right).$$

Conditional on $\beta(\lambda)$, as ζ_i determines $\text{sign}(W_i^{\text{S}\star})$ and B_i , the filtration $\{\mathcal{F}_j\}_{j=1}^m$ is a refined filtration of $\{\mathcal{G}_j\}_{j=1}^m$ in inverse time, i.e. $\mathcal{G}_j \subset \mathcal{F}_j$.

By Barber et al. (2015, 2019), J is a stopping time on $\{\mathcal{G}_j\}_{j=1}^m$ in inverse time, thus J is also a stopping time on the refined filtration $\{\mathcal{F}_j\}_{j=1}^m$ in inverse time. Furthermore, we will have the following supermartingale inequality which gives an upper bound on the expectation of Eq. (34).

Lemma B.2 (Lemma 3.3). *Consider the independent continuous random variables $\{\zeta_i\}_{i=1}^m$. Given any determined $\beta(\lambda)$, let $\{G_i\}_{i=1}^m$ be some Borel sets such that $B_i = 1\{\zeta_i \in G_i\}$ with $\mathbb{P}[B_i = 1] = \rho_i$. Let $\rho > 0$ satisfying $\rho \leq \min_i \{\rho_i\}$. Let J be a stopping time with respect to the filtration $\{\mathcal{F}_j\}_{j=1}^m$ in inverse time defined as*

$$\mathcal{F}_j = \sigma \left(\left\{ \sum_{i=1}^j B_{(i)}, \zeta_{(j+1)}, \dots, \zeta_{(m)} \right\} \right)$$

Then

$$\mathbb{E} \left[\frac{1+J}{1+B_{(1)}+B_{(2)}+\dots+B_{(J)}} \right] \leq \rho^{-1}.$$

Applying Lemma B.2 to Eq. (34), with the estimation that $\mathbb{P}[B_i = 1] \geq \rho = \frac{1}{2}$ for $i \in S_0$ by Lemma B.1, we will have the following inequality on $\mathcal{M}_{T_q^{\text{S}\star}}(W^{\text{S}\star})$ that

$$\mathbb{E} \left[\mathcal{M}_{T_q^{\text{S}\star}}(W^{\text{S}\star}) \right] = \mathbb{E} \left[\frac{\sum_{i \in S_0} 1\{W_i^{\text{S}\star} \geq T_q^{\text{S}\star}\}}{1 + \sum_{i \in S_0} 1\{W_i^{\text{S}\star} \leq -T_q^{\text{S}\star}\}} \right] \leq \rho^{-1} - 1 = 1, \quad (35)$$

Combining such results with Eq. (31) and Eq. (32), and we will finish the proof.

B.2 Proof for Theorem 3.1: Case II

As a reminder of notations, $(\text{BC}\star, \text{S}\star)$ denotes an arbitrary element from $\{(\text{BC}, \text{S}), (\text{BC}\tau, \text{S}\tau)\}$. We will show in this part that Theorem 3.1 holds in the case of $W^{\text{BC}\star}$. First of all, following the standard steps in knockoffs as shown in Section B, bounding the FDR by q can be transferred to the problem of bounding $\mathbb{E} \left[\mathcal{M}_{T_q^{\text{BC}\star}}(W^{\text{BC}\star}) \right]$ by one where

$$\mathcal{M}_T(W^{\text{BC}\star}) = \frac{\sum_{i \in S_0} 1\{W_i^{\text{BC}\star} \geq T\}}{1 + \sum_{i \in S_0} 1\{W_i^{\text{BC}\star} \leq -T\}}. \quad (36)$$

However due to the failure of exchangeability, $\mathcal{M}_T(W^{BC*})$ is now no longer a supermartingale with stopping time T_q^{BC*} . To address this challenge, we are going to show that $\mathcal{M}_T(W^{S*})$ gives an upper bound of $\mathcal{M}_T(W^{BC*})$ and is associated with a supermartingale structure at the same time. Specifically, we will show the following properties:

- (a) $\mathcal{M}_T(W^{S*})$ provides an upper bound for $\mathcal{M}_T(W^{BC*})$, that $\mathcal{M}_T(W^{BC*}) \leq \mathcal{M}_T(W^{S*})$;
- (b) T_q^{BC*} induces a stopping time for the inverse martingale associated with $\mathcal{M}_T(W^{S*})$ which enables the application of upper bounds in Case I to Case II.

a) Upper Bound Property

Comparing the definition of W^{BC*} and the definition of W^{S*} , we have

1. for $W_i^{BC*} > 0$, $W_i^{BC*} = Z_i = W_i^{S*}$;
2. for $W_i^{BC*} < 0$, if $(BC*, S*) = (BC, S)$, $W_i^{BC*} = -\tilde{Z}_i \leq -Z_i = W_i^{S*}$;
3. for $W_i^{BC*} < 0$, if $(BC*, S*) = (BC\tau, S\tau)$, $W_i^{BC*} = -\tau(\tilde{Z})_i \leq -Z_i = W_i^{S*}$;
4. W_i^{BC*} shares the same sign with W_i^{S*} .

Therefore, $\{i \in S_0 : W_i^{BC*} \geq T\} = \{i \in S_0 : W_i^{S*} \geq T\}$, while $\{i \in S_0 : W_i^{S*} \leq -T\} \subset \{i \in S_0 : W_i^{BC*} \leq -T\}$, which further indicates

$$\mathcal{M}_T(W^{BC*}) = \frac{\sum_{i \in S_0} 1\{W_i^{BC*} \geq T\}}{1 + \sum_{i \in S_0} 1\{W_i^{BC*} \leq -T\}} \leq \frac{\sum_{i \in S_0} 1\{W_i^{S*} \geq T\}}{1 + \sum_{i \in S_0} 1\{W_i^{S*} \leq -T\}} =: \mathcal{M}_T(W^{S*}). \quad (37)$$

Thus $\mathcal{M}_T(W^{S*})$ offers an upper bound for $\mathcal{M}_T(W^{BC*})$.

b) Stopping Time and Supermartingale Inequalities

To apply the supermartingale inequality in Lemma B.2, we will need to check that T_q^{BC*} defined on W^{BC*} can be induced to a stopping time associated with $\mathcal{M}_T(W^{S*})$ with respect to a proper filtration.

For shorthand notations, we rearrange the index on of W^{S*} , such that $|W_{(1)}^{S*}| \geq |W_{(2)}^{S*}| \geq \dots \geq |W_{(m^*)}^{S*}|$, and $\{(1), (2), \dots, (m^*)\} = S_0$, where $m^* = |S_0| \leq m$. Further denote $B_{(i)} = 1\{W_{(i)}^{S*} < 0\}$, then there holds

$$\begin{aligned} \frac{\sum_{i \in S_0} 1\{W_i^{S*} \geq T_q^{BC*}\}}{1 + \sum_{i \in S_0} 1\{W_i^{S*} \leq -T_q^{BC*}\}} &= \frac{1 + \sum_{i \in S_0} 1\{|W_i^{S*}| \geq T_q^{BC*}\}}{1 + \sum_{i \in S_0} 1\{|W_i^{S*}| \geq T_q^{BC*}, W_i^{S*} < 0\}} - 1, \\ &= \frac{1 + J}{1 + B_{(1)} + B_{(2)} + \dots + B_{(J)}} - 1, \end{aligned} \quad (38)$$

where $J \leq m^*$ is defined to be the index satisfying

$$|W_{(1)}^{S\star}| \geq |W_{(2)}^{S\star}| \geq \cdots \geq |W_{(J)}^{S\star}| \geq T_q^{BC\star} > |W_{(J+1)}^{S\star}| \geq \cdots \geq |W_{(m^*)}^{S\star}|,$$

in other words, $J = \operatorname{argmax}_{k \leq m^*} \{|W_{(k)}^{S\star}| \geq T_q^{BC\star}\}$. It can be shown $\mathcal{F}^{S\star}(T)$ is a refined filtration of $\mathcal{F}^{BC\star}(T)$, i.e. $\mathcal{F}^{BC\star}(T) \subseteq \mathcal{F}^{S\star}(T)$ in a similar way as discussed in Section 3. Rigorously speaking, we will have the following lemma showing that J is also a stopping time in inverse time with respect to the filtration \mathcal{F} associated with $W^{S\star}$.

Lemma B.3 (Lemma 3.4). *For any determined $\beta(\lambda)$, $J = \max_{i \leq m^*} \{|W_{(i)}^{S\star}| \geq T_q^{BC\star}\}$ is a stopping time with respect to the filtration $\{\mathcal{F}_j\}_{j=1}^m$ in inverse time defined as*

$$\mathcal{F}_j = \sigma \left(\left\{ \sum_{i=1}^j B_{(i)}, \zeta_{(j+1)}, \dots, \zeta_{(m)} \right\} \right).$$

Then we can apply Lemma B.2 again. Specifically we will have the following inequality on $\mathcal{M}_{T_q^{BC\star}}(W^{BC\star})$ and $\mathcal{M}_{T_q^{BC\star}}(W^{S\star})$:

$$\mathbb{E} \left[\mathcal{M}_{T_q^{BC\star}}(W^{BC\star}) \right] \leq \mathbb{E} \left[\mathcal{M}_{T_q^{BC\star}}(W^{S\star}) \right] = \mathbb{E} \left[\frac{\sum_{i \in S_0} \mathbb{1}\{W_i^{S\star} \geq T_q^{BC\star}\}}{1 + \sum_{i \in S_0} \mathbb{1}\{W_i^{S\star} \leq -T_q^{BC\star}\}} \right] \leq 1, \quad (39)$$

which ends the proof.

C Proof for Key Lemmas

In this section, we will give proofs on Lemma 3.2 (Lemma B.1), Lemma 3.3 (Lemma B.2), and Lemma 3.4 (Lemma B.3) respectively. For shorthand notations, let $(BC\star, S\star)$ be any element from $\{(BC, S), (BC\tau, S\tau)\}$, where $W^{BC\tau}$ is defined in Section B for completeness.

In the proof for Lemma 3.2, we give detailed analysis on the KKT conditions (12), which provides a specific mapping from the value of ζ to $\operatorname{sign}(W^{S\star})$. Then one can get $\mathbb{P}[W^{S\star} < 0]$ from the probability measure on ζ .

In the proof for Lemma 3.3, we explicitly construct a decomposition in B_i similar with that in proof of Lemma 1 in Barber et al. (2019), based on the property that $B_i = \mathbb{1}\{\zeta_i \in G_i\}$ for some Borel set G_i . Such a decomposition enables us the desired result.

In the proof for Lemma 3.4, we apply the ideas of $\mathcal{F}^{BC}(T) \subseteq \mathcal{F}^S(T)$ introduced in Section 3 in a discrete form. We will show that such result holds for any choice of $(BC\star, S\star)$ in the proof.

C.1 Proof for Lemma 3.2 (Lemma B.1)

Note that by Eq. (6), there holds

$$\begin{aligned}\tilde{A}_{\gamma,1}^T \frac{X_2}{\sqrt{n_2}} + \tilde{A}_{\gamma,2}^T \frac{D}{\sqrt{\nu}} &= \tilde{A}_{\gamma}^T A_{\beta} = A_{\gamma}^T A_{\beta} = -\frac{D}{\nu}, \\ -\frac{\tilde{A}_{\gamma,2}^T}{\sqrt{\nu}} &= \tilde{A}_{\gamma}^T A_{\gamma} = A_{\gamma}^T A_{\gamma} - \text{diag}\{s\} = \frac{I_m}{\nu} - \text{diag}\{s\},\end{aligned}$$

where $\tilde{A}_{\gamma,1} \in \mathbb{R}^{n_2 \times m}$ is defined to be the matrix that takes first n_2 rows of \tilde{A}_{γ} and $\tilde{A}_{\gamma,2} \in \mathbb{R}^{m \times m}$ is defined to be the matrix that takes last m rows of \tilde{A}_{γ} . Therefore, there holds

$$\tilde{A}_{\gamma}^T \tilde{y} = \tilde{A}_{\gamma,1}^T \frac{X_2 \beta^* + \varepsilon_2}{\sqrt{n_2}} = -\text{diag}(s) \gamma^* + \frac{\tilde{A}_{\gamma,1}^T}{\sqrt{n_2}} \varepsilon_2, \quad (40)$$

where ε_2 is the last n_2 rows of ε .

Note from Eq. (33a) that $\gamma(\lambda)$ is only correlated with $\beta(\lambda)$, which suggests that Z is determined by $\beta(\lambda)$. We will show by the following lemmas that $\text{sign}(W^{\text{S}\star})$ is determined by ζ conditional on a determined $\beta(\lambda)$ for $\text{S}\star = \text{S}$ and $\text{S}\star = \text{S}\tau$ respectively.

Lemma C.1. *For any determined $\beta(\lambda)$, there exists a vector $c(\nu) \in \mathbb{R}^m$, s.t.*

$$\{-c(\nu)_i < r_i \zeta_i < 0\} \subset \{W_i^{\text{S}} > 0\}, \quad \{r_i \zeta_i < -c(\nu)_i\} \cup \{r_i \zeta_i > 0\} \subset \{W_i^{\text{S}} > 0\}$$

where $r_i := \lim_{\lambda \rightarrow Z_i^-} \text{sign} \gamma_i(\lambda)$.

Proof. We show that $c(\nu)_i = \min_{\lambda \geq Z_i} (r_i [D\beta(\lambda)]_i \nu^{-1} + \lambda)$ is the proper choice of $c(\nu)$. The existence of such minimum is ensured by the continuity of $r_i [D\beta(\lambda)]_i \nu^{-1} + \lambda$, and the fact that $r_i [D\beta(\lambda)]_i \nu^{-1} + \lambda \rightarrow \infty$ for any ν as $\lambda \rightarrow \infty$.

1) $\{-c(\nu)_i < r_i \zeta_i < 0\} \subset \{W_i^{\text{S}} > 0\}$.

Suppose that $-c(\nu)_i < r_i \zeta_i < 0$. From Eq. (33a) and (33b), for $\lambda > Z_i$, there holds

$$\begin{aligned}r_i \lambda \tilde{\rho}_i(\lambda) + r_i \frac{\tilde{\gamma}_i(\lambda)}{\nu} &= r_i [D\beta(\lambda)]_i \nu^{-1} + r_i \zeta_i < r_i [D\beta(\lambda)]_i \nu^{-1} = r_i \lambda \rho_i(\lambda) \leq \lambda, \\ r_i \lambda \tilde{\rho}_i(\lambda) + r_i \frac{\tilde{\gamma}_i(\lambda)}{\nu} &= r_i [D\beta(\lambda)]_i \nu^{-1} + r_i \zeta_i > -\lambda.\end{aligned}$$

Combining these points together, for $\lambda > Z_i$, there holds $\tilde{\gamma}_i(\lambda) = 0$. By continuity of $\tilde{\gamma}_i(\lambda)$, this further means $\tilde{Z}_i < Z_i$ and $W_i^{\text{S}} > 0$.

2) $\{r_i\zeta_i < -c(\nu)_i\} \cup \{r_i\zeta_i > 0\} \subset \{W_i^S > 0\}$.

For the case that $r_i\zeta_i > 0$, for $\lambda = Z_i -$, there holds $r_i\rho_i(\lambda) = 1$ and $r_i\gamma(\lambda)_i > 0$. From (33a) - (33b) and $|r_i\tilde{\rho}_i(\lambda)| \leq 1$, there further holds

$$\begin{aligned} 0 \leq \lambda r_i\rho_i(\lambda) - \lambda r_i\tilde{\rho}_i(\lambda) &= r_i \frac{\tilde{\gamma}_i(\lambda)}{\nu} - r_i \frac{\gamma_i(\lambda)}{\nu} - r_i\zeta_i, \\ &< r_i \frac{\tilde{\gamma}_i(\lambda)}{\nu} - r_i\zeta_i. \end{aligned}$$

Therefore $r_i\tilde{\gamma}_i(\lambda) > r_i\zeta_i\nu$. By continuity of $\tilde{\gamma}_i(\lambda)$, there further holds $\tilde{Z}_i > Z_i$ and $W_i < 0$.

For the case that $r_i\zeta_i < -c(\nu)_i$, take $\lambda = \operatorname{argmin}_{t \geq Z_i} (r_i[D\beta(t)]_i\nu^{-1} + t)$, there holds

$$r_i\lambda\tilde{\rho}_i(\lambda) + r_i \frac{\tilde{\gamma}_i(\lambda)}{\nu} = r_i[D\beta(\lambda)]_i\nu^{-1} + r_i\zeta_i < -\lambda.$$

Therefore by continuity of $\tilde{\gamma}_i(\lambda)$, $\tilde{Z}_i > \lambda \geq Z_i$, which means $W_i^S < 0$. This ends the proof. \square

Lemma C.2. *Consider an arbitrary determined $\beta(\lambda)$. For all $i \in S_0$, there holds*

$$\{r_i\zeta_i < 0\} \subset \{W_i^{S\tau} > 0\}, \quad \{r_i\zeta_i > 0\} \subset \{W_i^{S\tau} > 0\}$$

Proof. We prove this lemma by exploring properties on KKT conditions of split knock-offs. From Equation (33a) - (33b), for $i \in S_0$, there holds

$$\lambda\rho_i(\lambda) - \lambda\tilde{\rho}_i(\lambda) = \frac{\tilde{\gamma}_i(\lambda)}{\nu} - \frac{\gamma_i(\lambda)}{\nu} - \zeta_i. \quad (41)$$

Without further statements, we consider $i \in S_0$ in this proof. For simplicity, we only consider the case of $r_i = 1$, since the symmetric case when $r_i = -1$ can be proved similarly.

1) $\{r_i\zeta_i < 0\} \subset \{W_i^{S\tau} > 0\}$.

For the case $r_i\zeta_i < 0$, there holds $\zeta_i < 0$. If in this case $W_i^{S\tau} \leq 0$, then there holds $\tilde{r}_i = r_i = 1$ and $\tilde{Z}_i \geq Z_i$. Take $\lambda = \tilde{Z}_i$, there holds $\lambda\tilde{\rho}_i(\lambda) = \lambda \geq \lambda\rho_i(\lambda)$, $\tilde{\gamma}_i(\lambda) = \gamma_i(\lambda) = 0$. Therefore, from Equation (41), there holds

$$0 \geq \lambda\rho_i(\lambda) - \lambda\tilde{\rho}_i(\lambda) = \frac{\tilde{\gamma}_i(\lambda)}{\nu} - \frac{\gamma_i(\lambda)}{\nu} - \zeta_i = -\zeta_i,$$

which means $\zeta_i \geq 0$ and leads to contradiction. Thus $W_i^{S\tau} > 0$.

2) $\{r_i \zeta_i > 0\} \subset \{W_i^{S\tau} < 0\}$.

For the case $r_i \zeta_i > 0$, there holds $\zeta_i > 0$. Take $\lambda = Z_i$, then there holds $\lambda \rho_i(\lambda) = \lambda \geq \lambda \tilde{\rho}_i(\lambda)$ and $\gamma_i(\lambda) \geq 0$. Therefore, from Equation (41), there holds

$$\begin{aligned} 0 \leq \lambda \rho_i(\lambda) - \lambda \tilde{\rho}_i(\lambda) &= \frac{\tilde{\gamma}_i(\lambda)}{\nu} - \frac{\gamma_i(\lambda)}{\nu} - \zeta_i, \\ &\leq \frac{\tilde{\gamma}_i(\lambda)}{\nu} - \zeta_i. \end{aligned}$$

This inequality means $\tilde{\gamma}_i(Z_i) \geq \nu \zeta_i > 0$, and therefore by the continuity of $\tilde{\gamma}_i$, $\tilde{Z}_i > Z_i$. Moreover, for $\lambda > Z_i$, there holds $\gamma_i(\lambda) = 0$. From Equation (41), there holds

$$-\lambda < \lambda \rho_i(\lambda) + \zeta = \lambda \tilde{\rho}_i(\lambda) + \frac{\tilde{\gamma}_i(\lambda)}{\nu},$$

which means $\tilde{\gamma}_i(\lambda) \geq 0$ for $\lambda > Z_i$. This further implies $\tilde{r}_i = r_i = 1$. Thus $W^{S\tau} < 0$. \square

Combining Lemma C.1 and Lemma C.2, we will give the following corollary.

Corollary C.2.1. *For any determined $\beta(\lambda)$, let $B_i := 1\{W_i^{S\star} < 0\}$, then B_i are some independent Bernoulli random variables.*

Proof. Note that by Eq. (6), there holds

$$\begin{aligned} \tilde{A}_{\gamma,1}^T \tilde{A}_{\gamma,1} + \tilde{A}_{\gamma,2}^T \tilde{A}_{\gamma,2} &= \tilde{A}_{\gamma}^T \tilde{A}_{\gamma} = A_{\gamma}^T A_{\gamma} = \frac{I_m}{\nu}, \\ -\frac{\tilde{A}_{\gamma,2}^T}{\sqrt{\nu}} &= \tilde{A}_{\gamma}^T A_{\gamma} = A_{\gamma}^T A_{\gamma} - \text{diag}\{s\} = \frac{I_m}{\nu} - \text{diag}\{s\}, \end{aligned}$$

where $\tilde{A}_{\gamma,2} \in \mathbb{R}^{m \times m}$ is defined to be the matrix that takes last m rows of \tilde{A}_{γ} . Therefore, there holds

$$\tilde{A}_{\gamma,1}^T \tilde{A}_{\gamma,1} = \text{diag}(s)(2I_m - \text{diag}(s)\nu),$$

and

$$\zeta \sim \mathcal{N} \left(-\text{diag}(s)\gamma^*, \frac{1}{n_2} \text{diag}(s)(2I_m - \text{diag}(s)\nu)\sigma^2 \right), \quad (42)$$

is some independent Gaussian random variables. Combining with Lemma C.1, Lemma C.2, and the fact that r is determined by $\beta(\lambda)$, we will get our desired result. \square

Then it remains to show that for $i \in S_0$, there holds $\mathbb{P}[B_i = 1] \geq \rho(\nu) \geq \frac{1}{2}$ to prove Lemma B.1.

Proof. First, from Lemma C.1, there holds $\{r_i \zeta_i > 0\} \subset \{W_i^S < 0\}$, where for $i \in S_0$,

$$\zeta_i \sim \mathcal{N} \left(0, \frac{1}{n_2} s_i (2 - s_i \nu) \sigma^2 \right).$$

Thus $\mathbb{P}[W_i^S < 0] \leq \mathbb{P}[r_i \zeta_i > 0] = \frac{1}{2}$. Meanwhile, from Lemma C.2, $\mathbb{P}[W_i^{S\tau} < 0] = \mathbb{P}[r_i \zeta_i > 0] = \frac{1}{2}$ for $i \in S_0$. Particularly, By Lemma C.1 and Lemma C.2, there holds $\mathbb{P}[W_i^{S\star} = 0] \leq \mathbb{P}[r_i \zeta_i = 0] + \mathbb{P}[r_i \zeta_i = c(\nu)] = 0$. This ends the proof. \square

C.2 Proof for Lemma 3.3 (Lemma B.2)

Proof. We start with the following constructions. For each i , we divide the space \mathbb{R} into 4 disjoint Borel sets, $\mathbb{R} = A_1^i \cup A_2^i \cup A_3^i \cup A_4^i$, with $G_i = A_2^i \cup A_3^i \cup A_4^i$, and

1. $\mathbb{P}[\zeta_i \in A_1^i] = 1 - \rho_i$;
2. $\mathbb{P}[\zeta_i \in A_2^i] = \rho \frac{1 - \rho_i}{1 - \rho}$;
3. $\mathbb{P}[\zeta_i \in A_3^i] = \rho \frac{\rho_i - \rho}{1 - \rho}$;
4. $\mathbb{P}[\zeta_i \in A_4^i] = \rho_i - \rho$.

The existence of such division is ensured by $1 - \rho_i + \rho \frac{1 - \rho_i}{1 - \rho} + \rho \frac{\rho_i - \rho}{1 - \rho} + \rho_i - \rho = 1$. Take $U_i = A_1^i \cup A_2^i$, and $V_i = A_2^i \cup A_3^i$ for each i .

Then we define $Q_i = 1\{\zeta_i \in V_i\}$ and a random set $A := \{i : \zeta_i \in U_i\}$. Thus

$$\begin{aligned} Q_i \cdot 1\{i \in A\} + 1\{i \notin A\} &= 1\{\{\zeta_i \in V_i \cap U_i\} \cup \{\zeta_i \in U_i^C\}\}, \\ &= 1\{\{\zeta_i \in A_2^i\} \cup \{\zeta_i \in A_3^i \cup A_4^i\}\}, \\ &= 1\{\zeta_i \in G_i\} = B_i. \end{aligned}$$

Therefore

$$\begin{aligned} \frac{1+J}{1+B_{(1)}+B_{(2)}+\cdots+B_{(J)}} &= \frac{1+|\{i \leq J : (i) \in A\}| + |\{i \leq J : (i) \notin A\}|}{1+\sum_{i \leq J, (i) \in A} Q_{(i)} + |\{i \leq J : (i) \notin A\}|}, \\ &\leq \frac{1+|\{i \leq J : (i) \in A\}|}{1+\sum_{i \leq J, (i) \in A} Q_{(i)}}, \end{aligned} \tag{43}$$

where the last step is by the inequality $\frac{a+c}{b+c} \leq \frac{a}{b}$ whenever $0 < b \leq a$ and $c \geq 0$.

Let $\tilde{Q}_i = Q_i \cdot 1\{i \in A\}$, and define

$$\mathcal{F}'_j = \sigma \left(\left\{ \sum_{i=1}^j \tilde{Q}_{(i)}, \zeta_{(j+1)}, \dots, \zeta_{(m)}, A \right\} \right),$$

then clearly $\{\mathcal{F}'_j\}_{j=1}^m$ is a filtration in inverse time, and $\mathcal{F}_j \subset \mathcal{F}'_j$, thus J is also a stopping time on \mathcal{F}'_j . Moreover, note that by definition

$$\begin{aligned} \mathbb{P}[Q_i = 1 | i \in A] &= \mathbb{P}[\zeta_i \in V_i | \zeta_i \in U_i] = \frac{\mathbb{P}[A_2^i]}{\mathbb{P}[A_1^i \cup A_2^i]} = \rho = \mathbb{P}[Q_i = 1], \\ \mathbb{P}[Q_i = 1 | i \notin A] &= \mathbb{P}[\zeta_i \in V_i | \zeta_i \notin U_i] = \frac{\mathbb{P}[A_3^i]}{\mathbb{P}[A_3^i \cup A_4^i]} = \rho = \mathbb{P}[Q_i = 1]. \end{aligned}$$

Such a observation combining with the the independence on ζ_i means that conditional on any fixed A , Q_i are i.i.d. Bernoulli random variables with parameter ρ . This further suggests that Q_i as i.i.d. Bernoulli random variables with parameter ρ , and are

independent from A . Such a property suggests that Q_i are exchangeable conditional on any fixed A , then by Barber et al. (2015, 2019), there holds

$$\mathbb{E} \left[\frac{1 + |\{i \leq J : (i) \in A\}|}{1 + \sum_{i \leq J, (i) \in A} Q_{(i)}} \middle| A \right] \leq \rho^{-1}.$$

Taking expectation over A , and we will get our desired result. \square

C.3 Proof for Lemma 3.4 (Lemma B.3)

Proof. For shorthand notations, let $(BC\star, S\star)$ be an arbitrary element from $\{(BC, S), (BC\tau, S\tau)\}$, where $W^{BC\tau}$ is defined in Section B for completeness. By definition of stopping time, we need to show that $\{J \leq k\} \in \mathcal{F}_k$ for $k \leq m^*$. We first validate that $\{\mathcal{F}_j\}_{j=1}^m$ is indeed a filtration in inverse time. By Eq. (33), for any determined $\beta(\lambda)$, $\zeta_{(i)}$ will determine $W_{(i)}^{BC\star}$ as well as $W_{(i)}^{S\star}$ for all i , thus determine $B_{(i)}$ and such a fact validates our claim. Furthermore, by the fact that $W^{BC\star}$ and $W^{S\star}$ share the same sign, we note that from the definitions of the filtration \mathcal{F} and $T_q^{BC\star}$:

- \mathcal{F}_k includes $\{W_{(i)}^{BC\star} : i > k\}$, $V_s^-(k) := \#\{W_{(i)}^{BC\star} < 0, i \leq k\}$, and $V_s^+(k) := \#\{W_{(i)}^{BC\star} > 0, i \leq k\} = k - V_s^-(k)$.
- the event $\{J \leq k\}$ is defined by, for all l such that $|W_{(l)}^{BC\star}| < |W_{(k)}^{S\star}|$

$$\frac{|\{i : W_{(i)}^{BC\star} \leq -|W_{(l)}^{BC\star}|\}|}{1 \vee |\{i : W_{(i)}^{BC\star} \geq |W_{(l)}^{BC\star}|\}|} > q,$$

i.e. decided by $\#\{i : W_{(i)}^{BC\star} \leq -|W_{(l)}^{BC\star}|\}$ and $\#\{i : W_{(i)}^{BC\star} \geq |W_{(l)}^{BC\star}|\}$. Note that for $l \leq k$, $|W_{(l)}^{BC\star}| \geq |W_{(l)}^{S\star}| \geq |W_{(k)}^{S\star}|$, therefore, the l such that $|W_{(l)}^{BC\star}| < |W_{(k)}^{S\star}|$ must satisfy $l > k$. Moreover, for $l > k$, $W_{(l)}^{BC\star} \in \{W_{(i)}^{BC\star} : i > k\} \subset \mathcal{F}_k$, thus all possible choices of $W_{(l)}^{BC\star}$ is already known under \mathcal{F}_k .

Hence it suffices to show that, for all $l > k$ such that $|W_{(l)}^{BC\star}| < |W_{(k)}^{S\star}|$, \mathcal{F}_k includes

$$\#\{i : W_{(i)}^{BC\star} \leq -|W_{(l)}^{BC\star}|\} \text{ and } \#\{i : W_{(i)}^{BC\star} \geq |W_{(l)}^{BC\star}|\}.$$

To see this, the first set is decomposed by

$$\begin{aligned} & \#\{W_{(i)}^{BC\star} \leq -|W_{(l)}^{BC\star}|\} \\ &= \#\{W_{(i)}^{BC\star} \leq -|W_{(l)}^{BC\star}|, i \leq k\} + \#\{W_{(i)}^{BC\star} \leq -|W_{(l)}^{BC\star}|, i > k\}, \\ &= \#\{W_{(i)}^{BC\star} < 0, i \leq k\} + \#\{W_{(i)}^{BC\star} \leq -|W_{(l)}^{BC\star}|, i > k\}. \end{aligned}$$

The last step is by for $i \leq k$, $|W_{(i)}^{BC\star}| \geq |W_{(i)}^{S\star}| \geq |W_{(k)}^{S\star}| > |W_{(l)}^{BC\star}|$. Here the first part is equal to $V_s^-(k) := \#\{W_{(i)}^{BC\star} < 0, i \leq k\}$, the second part is determined by

$\{W_{(i)}^{\text{BC}\star}, i > k\}$, both of which are in the σ -field of \mathcal{F}_k . This shows that \mathcal{F}_k includes $\#\{i : W_{(i)}^{\text{BC}\star} \leq -|W_{(l)}^{\text{BC}\star}|\}$. Similarly, the second set is decomposed by

$$\begin{aligned} & \#\{i : W_{(i)}^{\text{BC}\star} \geq |W_{(l)}^{\text{BC}\star}|\} \\ &= \#\{i : W_{(i)}^{\text{BC}\star} \geq |W_{(l)}^{\text{BC}\star}|, i \leq k\} + \#\{i : W_{(i)}^{\text{BC}\star} \geq |W_{(l)}^{\text{BC}\star}|, i > k\}, \\ &= \#\{i : W_{(i)}^{\text{BC}\star} > 0, i \leq k\} + \#\{i : W_{(i)}^{\text{BC}\star} \geq |W_{(l)}^{\text{BC}\star}|, i > k\}, \end{aligned}$$

where last step is by for $i \leq k$, $|W_{(i)}^{\text{BC}\star}| \geq |W_{(i)}^{\text{S}\star}| \geq |W_{(k)}^{\text{S}\star}| > |W_{(l)}^{\text{BC}\star}|$. The first part is equal to $V_s^+(k) = \#\{W_{(i)}^{\text{BC}\star} > 0, i \leq k\}$ and the second part is determined by $\{W_{(i)}^{\text{BC}\star} : i > k\}$, both of which are in the σ -field of \mathcal{F}_k . Therefore \mathcal{F}_k includes $\#\{i : W_{(i)}^{\text{BC}\star} \geq |W_{(l)}^{\text{BC}\star}|\}$. This finishes the proof. \square

D Proof for Theorem 4.1

In this section, we approach the model selection consistency problem by constructing Primal-Dual Witness (PDW) of Split LASSO regularization paths, following the same treatment in the traditional LASSO problem (Wainwright, 2009) and Split Linearized Bregman Iterations (Huang et al., 2016, 2020). We first introduce the successful Primal-Dual Witness which has a unique solution of Split LASSO; then we introduce the incoherence condition for Split LASSO and establish the no-false-positive and sign consistency of Split LASSO regularization path, i.e. Theorem 4.1.

The set of witness $(\hat{\beta}^\lambda, \hat{\gamma}^\lambda, \hat{\rho}^\lambda) \in \mathbb{R}^p \times \mathbb{R}^m \times \mathbb{R}^m$ is constructed in the following way:

1. First, we set $\hat{\gamma}_{S_0}^\lambda = 0$, and obtain $(\hat{\beta}^\lambda, \hat{\gamma}_{S_1}^\lambda) \in \mathbb{R}^p \times \mathbb{R}^{|S_1|}$ by solving

$$(\hat{\beta}^\lambda, \hat{\gamma}_{S_1}^\lambda) = \underset{(\beta, \gamma_{S_1})}{\operatorname{argmin}} \left\{ \frac{1}{2n} \|y - X\beta\|_2^2 + \frac{1}{2\nu} \|D\beta - \gamma\|_2^2 + \lambda \|\gamma_{S_1}\|_1 \right\}. \quad (44)$$

2. Second, we choose $\hat{\rho}_{S_1}^\lambda = \partial \|\hat{\gamma}_{S_1}^\lambda\|_1$ as the subgradient of $\|\hat{\gamma}_{S_1}^\lambda\|_1$.
3. Third, for no-false-positive, we solve for $\hat{\rho}_{S_0}^\lambda \in \mathbb{R}^{|S_0|}$ satisfying the KKT condition (45), and check whether or not the dual feasibility condition $|\hat{\rho}_j^\lambda| < 1$ for all $j \in S_0$ is satisfied.
4. Fourth, for model selection (sign) consistency, we check whether $\hat{\rho}_{S_1}^\lambda = \operatorname{sign}(\beta_{S_1}^*)$ is satisfied.

We start from the KKT conditions that an optimal solution of the Split LASSO problem (3) satisfies, as they will be commonly used throughout this section. The KKT conditions are

$$0 = -(\Sigma_X + L_D)\beta(\lambda) + \frac{D^T}{\nu} \gamma(\lambda) + \left\{ \Sigma_X \beta^* + \frac{X^T}{n} \varepsilon \right\}, \quad (45a)$$

$$\lambda \rho(\lambda) = \frac{D\beta(\lambda)}{\nu} - \frac{\gamma(\lambda)}{\nu}, \quad (45b)$$

where $\rho(\lambda) \in \partial\|\gamma(\lambda)\|_1$.

D.1 Primal-Dual Witness Property

In this section, we introduce the following lemma that gives the uniqueness property on the success of Primal-Dual Witness for Split LASSO problem.

Lemma D.1. *When the PDW succeed, if the subproblem (44) is strictly convex, the solution $(\hat{\beta}, \hat{\gamma})$ is the unique optimal solution for split LASSO.*

Proof. When PDW succeed, we have $\|\hat{\rho}_{S_0}\|_\infty < 1$, and therefore $(\hat{\beta}, \hat{\gamma})$ is a set of optimal solution, while $\hat{\rho}$ is in the subgradient of $\|\hat{\gamma}\|_1$. Let $(\tilde{\beta}, \tilde{\gamma})$ be any other optimal solution for Split LASSO. Denote

$$F(\beta, \gamma) = \frac{1}{2n} \|y - X\beta\|_2^2 + \frac{1}{2\nu} \|D\beta - \gamma\|_2^2.$$

Then there holds

$$F(\hat{\beta}, \hat{\gamma}) + \lambda \langle \hat{\rho}, \hat{\gamma} \rangle = F(\tilde{\beta}, \tilde{\gamma}) + \lambda \|\tilde{\gamma}\|_1,$$

which is

$$F(\hat{\beta}, \hat{\gamma}) - \lambda \langle \hat{\rho}, \hat{\gamma} \rangle - F(\tilde{\beta}, \tilde{\gamma}) = \lambda(\|\tilde{\gamma}\|_1 - \langle \hat{\rho}, \tilde{\gamma} \rangle).$$

Also, by Equation (45), there holds $\frac{\partial F(\hat{\beta}, \hat{\gamma})}{\partial \hat{\beta}} = 0$, and $\frac{\partial F(\hat{\beta}, \hat{\gamma})}{\partial \hat{\gamma}} = -\lambda \hat{\rho}$. Therefore

$$F(\hat{\beta}, \hat{\gamma}) + \langle \frac{\partial F(\hat{\beta}, \hat{\gamma})}{\partial \hat{\gamma}}, \tilde{\gamma} - \hat{\gamma} \rangle + \langle \frac{\partial F(\hat{\beta}, \hat{\gamma})}{\partial \hat{\beta}}, \tilde{\beta} - \hat{\beta} \rangle - F(\tilde{\beta}, \tilde{\gamma}) = \lambda(\|\tilde{\gamma}\|_1 - \langle \hat{\rho}, \tilde{\gamma} \rangle). \quad (46)$$

Since F is convex, left hand side of Equation (46) is non-positive, then there holds

$$\|\tilde{\gamma}\|_1 \leq \langle \hat{\rho}, \tilde{\gamma} \rangle.$$

Since $|\hat{\rho}_{S_0}| < 1$, there holds $\tilde{\gamma}_{S_0} = 0$. Therefore $(\tilde{\beta}, \tilde{\gamma})$ is also an optimal solution for the subproblem (44). If the subproblem (44) is strictly convex, then $(\hat{\beta}, \hat{\gamma})$ is the only solution for split LASSO. \square

D.2 Incoherence Condition and Path Consistency

In this section, We first show on how we can get the incoherence condition and then we give the proof for Theorem 4.1.

From $D[\Sigma_X + L_D]^{-1} \times$ Equation (45a) + $\nu \times$ Equation (45b), and the fact that $\gamma^* = D\beta^*$, there holds

$$\begin{aligned}\lambda\nu\hat{\rho} &= -\hat{\gamma} + \frac{D[\Sigma_X + L_D]^{-1}D^T\hat{\gamma}}{\nu} + D[\Sigma_X + L_D]^{-1}(\Sigma_X + L_D - L_D)\beta^* + \dots \\ &\quad \dots + D[\Sigma_X + L_D]^{-1}\frac{X^T}{n}\varepsilon, \\ &= -H_\nu(\hat{\gamma} - \gamma^*) + \omega,\end{aligned}$$

where $H_\nu = I_m - \frac{D[\Sigma_X + L_D]^{-1}D^T}{\nu}$, and $\omega = D[\Sigma_X + L_D]^{-1}\frac{X^T}{n}\varepsilon$. Define H_ν^{11} to be the covariance matrix for S_1 , H_ν^{00} to be the covariance matrix for S_0 , and H_ν^{10} , H_ν^{01} to be the covariance matrix between S_1 and S_0 , there holds

$$\lambda\nu \begin{bmatrix} \hat{\rho}_{S_1} \\ \hat{\rho}_{S_0} \end{bmatrix} = - \begin{bmatrix} H_\nu^{11} & H_\nu^{10} \\ H_\nu^{01} & H_\nu^{00} \end{bmatrix} \begin{bmatrix} \hat{\gamma}_{S_1} - \gamma_{S_1}^* \\ 0_{S_0} \end{bmatrix} + \begin{bmatrix} \omega_{S_1} \\ \omega_{S_0} \end{bmatrix},$$

which means

$$\lambda\nu\hat{\rho}_{S_1} = -H_\nu^{11}(\hat{\gamma}_{S_1} - \gamma_{S_1}^*) + \omega_{S_1}, \quad (47a)$$

$$\lambda\nu\hat{\rho}_{S_0} = -H_\nu^{01}(\hat{\gamma}_{S_1} - \gamma_{S_1}^*) + \omega_{S_0}. \quad (47b)$$

Assume that H_ν^{11} is reversible and solve $\hat{\gamma}_{S_1} - \gamma_{S_1}^*$ from Equation (47a), there holds

$$\hat{\gamma}_{S_1} - \gamma_{S_1}^* = -\lambda\nu[H_\nu^{11}]^{-1}\hat{\rho}_{S_1} + [H_\nu^{11}]^{-1}\omega_{S_1}. \quad (48)$$

Then, plugging Equation (48) into Equation (47b), there holds

$$\hat{\rho}_{S_0} = H_\nu^{01}[H_\nu^{11}]^{-1}\hat{\rho}_{S_1} + \frac{1}{\lambda\nu}\{\omega_{S_0} - H_\nu^{01}[H_\nu^{11}]^{-1}\omega_{S_1}\}. \quad (49)$$

Then we can give the Incoherence Condition (17) from Equation (49). Below, we are going to give the proof for Theorem 4.1.

Proof of Theorem 4.1.

1) From Equation (49) and Incoherence Condition (17), there holds

$$\begin{aligned}\|\hat{\rho}_{S_0}\|_\infty &\leq (1 - \chi) + \frac{1}{\lambda_n\nu}[\|\omega_{S_0}\|_\infty + (1 - \chi)\|\omega_{S_1}\|_\infty], \\ &\leq (1 - \chi) + \frac{1}{\lambda_n} \left\| \frac{\omega}{\nu} \right\|_\infty.\end{aligned}$$

Recall that $\omega = D[\Sigma_X + L_D]^{-1}\frac{X^T}{n}\varepsilon$, therefore $\frac{\omega_i}{\nu} = \frac{1}{\nu}D_i[\Sigma_X + L_D]^{-1}\frac{X^T}{n}\varepsilon$ is a Gaussian random variable with variance

$$\begin{aligned}&\frac{1}{\nu} \frac{\sigma^2}{n} D_{i,\cdot}[\Sigma_X + L_D]^{-1} \Sigma_X [\Sigma_X + L_D]^{-1} D_{i,\cdot}^T \\ &\leq \frac{1}{\nu} \frac{\sigma^2}{n} D_{i,\cdot}[\Sigma_X + L_D]^{-1} D_{i,\cdot}^T \leq \frac{\sigma^2}{n}.\end{aligned}$$

Therefore

$$\mathbb{P}\left(\left\|\frac{\omega}{\lambda_n \nu}\right\|_{\infty} \geq \frac{\chi}{2}\right) \leq 2m \exp\left(-\frac{\lambda_n^2 n \chi^2}{8\sigma^2}\right).$$

Moreover, by $\lambda_n > \frac{1}{\chi} \sqrt{\frac{\sigma^2 \log p}{n}}$, there holds

$$\mathbb{P}\left(\|\hat{\rho}_{S_0}\|_{\infty} > 1 - \frac{\chi}{2}\right) \leq 2e^{-2c_1 n \lambda_n^2},$$

for some constant c_1 .

2) From Equation (48), there holds

$$\|\hat{\gamma}_{S_1} - \gamma_{S_1}^*\|_{\infty} \leq \nu \lambda_n \| [H_{\nu}^{11}]^{-1} \|_{\infty} + \| [H_{\nu}^{11}]^{-1} \omega_{S_1} \|_{\infty}.$$

Note that the first term here is a deterministic term, therefore we only need to estimate the second term. Recall that $\|\frac{\sigma^2}{n} D[\Sigma_X + L_D]^{-1} \Sigma_X [\Sigma_X + L_D]^{-1} D^T\|_2 \leq \nu \frac{\sigma^2}{n}$, there holds

$$\mathbb{P}(\| [H_{\nu}^{11}]^{-1} \omega_{S_1} \|_{\infty} > \nu t) \leq 2 \exp\left(-\frac{t^2 C_{\min} n}{\sigma^2} + \log |S_1|\right),$$

which holds for any subgaussian noise of scale σ^2 . Take $t = 4\sigma \lambda_n / \sqrt{C_{\min}}$, and note that $8n\lambda_n^2 > \log m > \log |S_1|$, there holds

$$\mathbb{P}(\| [H_{\nu}^{11}]^{-1} \omega_{S_1} \|_{\infty} > \nu \frac{4\sigma \lambda_n}{\sqrt{C_{\min}}}) \leq 2 \exp(-c_2 \lambda_n^2 n).$$

After all, there holds

$$\|\hat{\gamma}_{S_1} - \gamma_{S_1}^*\|_{\infty} \leq \lambda_n \nu \left[\frac{4\sigma}{\sqrt{C_{\min}}} + \| [H_{\nu}^{11}]^{-1} \|_{\infty} \right],$$

with probability greater than $1 - 2 \exp(-c_2 \lambda_n^2 n)$. Therefore for $c = \max\{c_1, c_2\}$, if $\min_{i \in S_1} \gamma_i^* > \lambda_n \nu \left[\frac{4\sigma}{\sqrt{C_{\min}}} + \| [H_{\nu}^{11}]^{-1} \|_{\infty} \right]$, with probability greater than

$$1 - 4 \exp(-c \lambda_n^2 n),$$

$\hat{\gamma}$ recovers the support set of γ^* . □

E Supplementary Materials for Alzheimer's Disease Experiments

In this section, we provide more details regarding the experiments on Alzheimer's Disease. First, we provide the table for the names and abbreviations of Cerebrum Brain Regions. Second, we provide supplementary materials for experiments in Alzheimer's Disease in Section 6, where we plot the frequencies of the most frequently selected regions by Split Knockoffs in multiple data splits.

E.1 Names and Abbreviations in Automatic Anatomical Labeling (AAL) Atlas

In Figure 1, it illustrates the lesion regions and high contrast connections selected by Split Knockoff. In the graph, each vertex represents a Cerebrum brain region in Automatic Anatomical Labeling (AAL) atlas (Tzourio-Mazoyer et al., 2002), with abbreviations of each region marked in the vertex. A comparison table between the full region names and their abbreviations can be found in Table 4. Specially, vertices with a circle shape represent the left brain regions, while the ones with a square shape represent the right brain regions. There will be an edge connecting two vertices if and only if the respective two brain regions are adjacent.

E.2 Parameter Importance Index as Selection Frequency

In this section, we show the results of Split Knockoff under 100 different random splits of the dataset in Alzheimer’s Disease. The W statistics for Split Knockoff is taken to be $W^{S\tau}$ with $\beta(\lambda)$ is taken as a cross validation optimal estimator $\hat{\beta}_{\hat{\nu},\hat{\lambda}}$, with the ν for the feature significance and knockoff significance taken as $\hat{\nu}$. Throughout the random splitting, important regions and connections should be selected with high frequencies, while the false discoveries in each selection should have relatively low frequencies to be selected. We plot the top 10 most frequently selected regions/connections by Split Knockoff in 100 random data splits in Figure 4 and Figure 5, with abbreviations of each region marked in the figures. A comparison table between the full region names and their abbreviations can be found in Table 4.

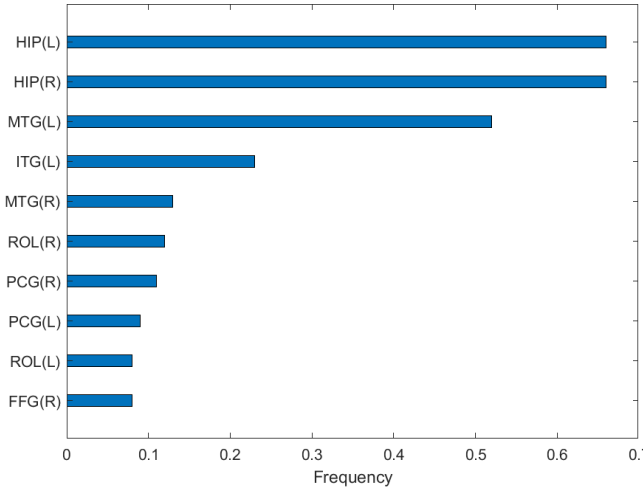


Figure 4: Top 10 most frequently selected lesion regions by Split Knockoff in 100 random data splits. The W statistics for Split Knockoff is taken to be $W^{S\tau}$, with $\beta(\lambda)$ taken as a fixed cross validation optimal estimator $\hat{\beta}_{\hat{\nu},\hat{\lambda}}$, with the ν in the calculation of feature significance and knockoff significance taken as $\hat{\nu}$.

Table 4: Names and Abbreviations for Cerebrum Brain Anatomical Regions

Region Name	Abbreviation
Precentral gyrus	PreCG
Superior frontal gyrus, dorsolateral	SFGdor
Superior frontal gyrus, orbital part	ORBsup
Middle frontal gyrus	MFG
Middle frontal gyrus, orbital part	ORBmid
Inferior frontal gyrus, opercular part	IFGoperc
Inferior frontal gyrus, triangular part	IFGtriang
Inferior frontal gyrus, orbital part	ORBinf
Rolandic operculum	ROL
Supplementary motor area	SMA
Olfactory cortex	OLF
Superior frontal gyrus, medial	SFGmed
Superior frontal gyrus, medial orbital	ORBsupmed
Gyrus rectus	REC
Insula	INS
Anterior cingulate and paracingulate gyri	ACG
Median cingulate and paracingulate gyri	MCG
Posterior cingulate gyrus	PCG
Hippocampus	HIP
Parahippocampal gyrus	PHG
Amygdala	AMYG
Calcarine fissure and surrounding cortex	CAL
Cuneus	CUN
Lingual gyrus	LING
Superior occipital gyrus	SOG
Middle occipital gyrus	MOG
Inferior occipital gyrus	IOG
Fusiform gyrus	FFG
Postcentral gyrus	PoCG
Superior parietal gyrus	SPG
Inferior parietal, but supramarginal and angular gyri	IPL
Supramarginal gyrus	SMG
Angular gyrus	ANG
Precuneus	PCUN
Paracentral lobule	PCL
Caudate nucleus	CAU
Lenticular nucleus putamen	PUT
Lenticular nucleus, pallidum	PAL
Thalamus	THA
Heschl gyrus	HES
Superior temporal gyrus	STG
Temporal pole: superior temporal gyrus	TPOsup
Middle temporal gyrus	MTG
Temporal pole: middle temporal gyrus	TPOmid
Inferior temporal gyrus	ITG

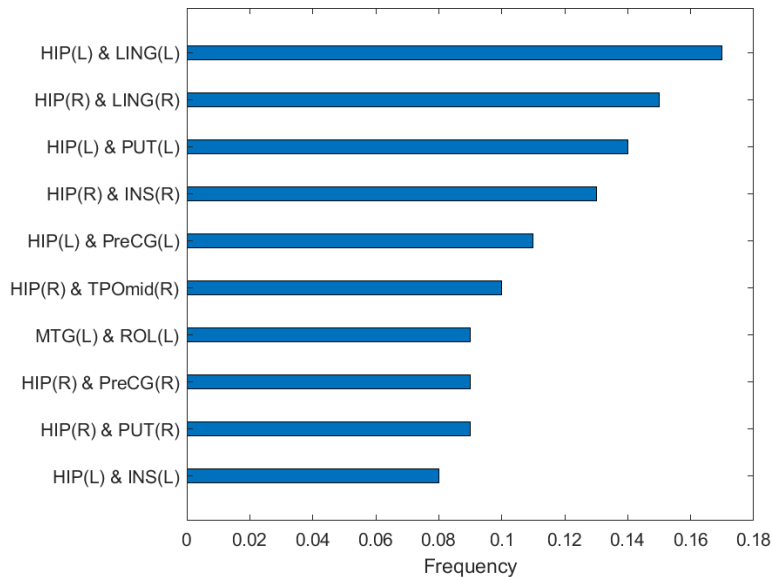


Figure 5: Top 10 most frequently selected connections of adjacent regions by Split Knockoff in 100 random data splits. The W statistics for Split Knockoff is taken to be $W^{S\tau}$, with $\beta(\lambda)$ taken as a fixed cross validation optimal estimator $\hat{\beta}_{\hat{\nu}, \hat{\lambda}}$, with the ν in the calculation of feature significance and knockoff significance taken as $\hat{\nu}$.